Green Synthesis of Sulfur-Containing Polymers by Carbon Disulfide-based Spontaneous Multicomponent Polymerization

Xu Chen,[a,b,d] Anjun Qin *[a,b] and Ben Zhong Tang *[b,c,e]

a. State Key Laboratory of Luminescent Materials and Devices, Guangdong Provincial Key Laboratory of Luminescence from Molecular Aggregates, South China University of Technology, Guangzhou 510640, China. E-mail: msqinaj@scut.edu.cn
b. Center for Aggregation-Induced Emission, AIE Institute, South China University of Technology, Guangzhou 510640, China.
c. School of Science and Engineering, Shenzhen Institute of Aggregate Science and Technology, The Chinese University of Hong Kong, Shenzhen (CUHK-Shenzhen), Guangdong 518172, China. E-mail: tangbenz@cuhk.edu.cn.
d. Department of Infectious Diseases, the Fifth Affiliated Hospital, Sun Yat-sen University, 52 East Meihua Road, Zhuhai 519000, Guangdong Province, China.
e. Hong Kong Branch of the Chinese National Engineering Research Centre for Tissue Restoration and Reconstruction, The Hong Kong University of Science & Technology, Kowloon 999077 Hong Kong, China.

Sulfur-containing polymers have gained much attention in polymer science due to their unique properties. Nevertheless, their preparation has posed considerable challenges, particularly in diversifying their structures and achieving highly efficient polymerizations. This is especially true for the polymers derived from CS_2, a readily available one-carbon (C1) feedstock, as their synthesis often necessitates harsh conditions or results in unexpected byproducts. In this work, we established a regio-selective and atom-economy spontaneous multicomponent polymerization based on carbonyl or ester group-activated internal alkynes, commercially available amines, and CS_2. Similar to the angled half lap joint of two plates in a scarf joint of in ancient Chinese tenon and mortise architecture, these internal ethynyl and amino groups can not readily react at room temperature. However, the addition of CS_2 acts as a "wedge," making the polymerization spontaneous and enabling the tight linkage and extension of these functional groups into stable polymer chains. The sulfur-containing polymers with satisfactory weight-average molecular weights (up to 31 600) were produced in high yields (up to 97%). The resultant polymers exhibit exceptional characteristics, including high refractive indices (up to 1.7471 at 632.8 nm), excellent light transmittance, and good film-forming capabilities. This work opens up a new avenue for the green and efficient synthesis of functional sulfur-containing polymers, using cost-effective CS_2 as starting material.

1. Introduction

Sulfur-containing polymers have gained much attention due to their superior electrical, optical, biological or mechanical properties, as well as distinct features like stabilization of free radicals or adhesion to heavy metals.[1-5] Condensation or ring-opening polymerizations are frequently used to prepare sulfur-containing polymers, such as poly(thioether)s, poly(thiourethane)s, poly(thiocarbonate)s, poly(trithiocarbonate)s, poly(thioester)s, and poly(sulfur-random-styrene)s.[6] Other reactions, such as copolymerization, are generally difficult to be used due to their poor selectivity.[7] Thus, it is still urgently necessary to expand the copolymerizations for preparing sulfur-containing polymers.

Abundant sulfur resources can be utilized as the monomers to prepare sulfur-containing polymers, including mercaptans, elemental sulfur, carbon disulfide (CS_2), carbonyl sulfide, and other sulfides.[8-11] Among them, CS_2 stands out as a readily available sulfur-rich one-carbon (C1) feedstock, which exists in a more transportable liquid form and shows a strong nucleophilicity.[12,13] However, the CS_2-based polymerizations are rather limited. The salenCrX-based system has grown to be the most popular catalyst for the copolymerization of episulfide/epoxide with CS_2 toward alternating polymers since it was first reported by Nozaki *et al.* in 2007.[14] The catalyst was further expanded by Darensbourg *et. al.* to heterogeneous zinc–cobalt double cyanide complex or homogeneous (salen)CrCl complex.[15]

Recently, a catalyst-free strategy was proposed for polythioureas preparation from diamines and CS_2 at 45 °C. However, the toxic hydrogen sulfide by-products were also generated.[16] Liu *et al*. also reported that CS_2, dihalides, and electron-withdrawing group-activated methylene derivatives could be polymerized using K_2CO_3 as a catalyst at room temperature. However, the reaction took up to 7 days to complete at a high monomer concentration.[17] Therefore, efficient polymerization, especially carried out in a spontaneous manner, of CS_2 at room temperature without initiators or catalysts remains a significant challenge.

Our groups have established a series of alkyne-based spontaneous click polymerizations, such as spontaneous amino-yne click polymerization, and regio- and stereoregular polymers were efficiently prepared.[18,19] The spontaneousness of the

reaction lies on the activation of the ethynyl groups by covalently connecting with electron-withdrawing ester, carbonyl, or sulfonyl groups.[20,21] However, the reactivity of activated alkynes greatly decrease compared with aforementioned terminal ones although they are more stable and could be synthesized more facilely. For example, the polymerization between activated internal alkynes and amines could not perform spontaneously and has to be conducted at elevated temperature or in the presence of catalysts.[22]

Taking cues from the design of the angled half lap joint of two plates in a scarf joint of ancient Chinese "tenon and mortise" architecture, where a wedge is essential for a secure connection, we speculated that the introduction of another monomeric component into the polymerization system might realize more efficient polymerization of activated internal alkynes.[23-29] In other word, the multicomponent polymerizations (MCPs) might be an ideal candidate although the one- and two-component polymerizations are well-established.[30-40] Indeed, it is reported that CS_2 is capable to efficiently react with secondary amines to form more nucleophilic dithiocarbamic acid derivatives,[41,42] which could react with activated internal alkynes in a spontaneous manner.[43] Thus, CS_2 acts as a "wedge" in this MCP. As a result, *S*-acylvinyl-*N*,*N*-dialkyl dithiocarbamates (ADDC) could be produced more facilely than previously reported reactions.[44-47]

Based on above reports and the "tenon and mortise" strategy, in this work, we successfully developed a spontaneous MCP of activated internal alkynes, secondary amines, and CS_2 (Scheme 1). The polymerization propagates smoothly at room temperature, and regio-regular poly(*S*-acylvinyl-*N*,*N*-dialkyldithiocarbamate)s (PADDCs) with weight-average molecular weights up to 31 600 were produced in high yields up to 97%. PADDCs show excellent processability and film-forming ability as well as high transparency and refractivity. Thus, in this work, we not only realize the polymerization of activated diynes and diamines spontaneously by introducing the third component of CS_2, but also made efficient use of the sulfur resources.

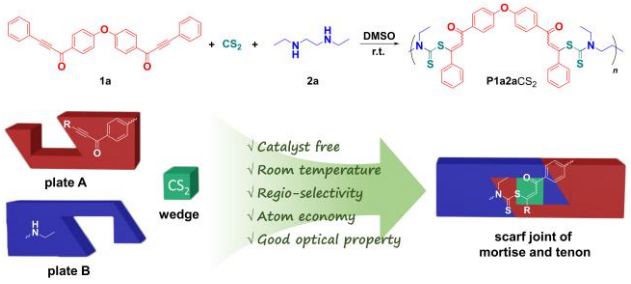

Scheme 1. Spontaneous polymerization of activated internal diyne **1a**, secondary diamine **2a** and CS_2. The two angled half lap joint plates of internal ethynyl and amino groups cannot spontaneously react, but with the assistance of a CS_2 "wedge", these two functional groups can be tightly linked to form stable polymer chains in a spontaneous manner.

2. Results and Discussion

2.1 Polymerization

The polymerization of activated internal diyne **1a**, secondary diamine **2a** and CS_2 (Scheme 1) was firstly conducted to understand the effects of solvent, monomer concentration, CS_2 equivalent and reaction time on its efficiency. The polymerization was initially conducted in chloroform (Table 1, entry 1), but the formed intermediate of dithiocarbamic acid derivative from **2a** and CS_2 was poorly soluble, making it difficult to generate final product. Hence, we screened solvents with higher polarity than chloroform, including tetrahydrofuran (THF), dimethyl sulfoxide (DMSO), *N*,*N*-dimethylformamide (DMF) and *N*,*N*-dimethylacetamide (DMAc), etc. for the polymerization (entries 2-5). Eventually, the polymer with the highest weight-average molecular weight (M_w) was obtained in DMSO, but the yield is lower than in DMAc, which might be due to the loss during the purification process. The use of a mixed solvent of DMSO and DMAc (entry 6) did not significantly improve the yield. Since the loss of product during extraction could be reduced with enhanced M_w, the green solvent of DMSO was selected as the optimal reaction solvent for further studies.

Table 1. Solvent effects on the polymerization of monomers **1a**, **2a** and CS_2.[a]

Entry	solvent	yield (%)	M_w [b]	$Đ$ [b]
1	$CHCl_3$	–	–	–
2	THF	29	1700	1.14
3	DMSO	54	7500	1.42
4	DMF	49	5900	1.29
5	DMAc	64	5500	1.27
6	DMAc+DMSO	57	7100	1.35

[a] Carried out under nitrogen at 25 °C for 12 h; [**1a**] = [**2a**] = 0.05 M, [CS_2] = 0.15 M. [b] Determined by gel-permeation chromatography (GPC) in DMF containing 0.05 M LiBr using linear polymethyl methacrylate (PMMA) for calibration.

Table 2. Effects of monomer concentrations on the spontaneous polymerization of monomers **1a**, **2a**, and CS_2.[a]

entry	[**1a**] and [**2a**] (mol/L)	yield (%)	M_w [b]	$Đ$ [b]
1	0.05	54	7500	1.42
2	0.1	53	8400	1.44
3	0.2	56	11 300	1.62
4	0.3	73	27 900	1.93
5	0.4	74	24 600	1.83

[a] Carried out under nitrogen in anhydrous DMSO at 25 °C for 12 h, [CS_2] = 3[**1a**] = 3[**2a**]. [b] Determined by gel-permeation chromatography (GPC) in DMF containing 0.05 M LiBr using linear PMMA for calibration.

Second, we studied the monomer concentration on the polymerization results. We further enhanced the monomer concentration to improve the M_w and yield of product because they are low when the polymerization was performed in a low concentration of 0.05 M (entry 1, Table 2). As shown in Table 2 (entries 2-5), polymers with significantly high M_w values were obtained when the monomer concentration was increased to 0.3 M. A further increase in the concentration to 0.4 M resulted

in a slight decrease of M_w of the product, which might be due to the uneven stirring of the high viscosity system[48]. Therefore, the optimal monomer concentration was selected to be 0.3 M.

Third, we varied the CS_2 content during the polymerization. The data listed in Table S1 revealed that the concentration of CS_2 does not significantly affect the efficiency of the polymerization. Using a 3-fold higher concentration of CS_2 compared to the other monomers is sufficient to ensure efficient propagation of the polymerization. Finally, the time course of the polymerization was followed (Table S2). The M_w values of the products increase gradually at the early reaction stage, and the highest M_w was recorded at 8 h. Continuing the reaction for a longer duration did not yield a higher M_w value. Thus, the optimized polymerization reaction conditions were obtained as 0.3 M **1a** with the feed ratio of **1a**:**2a**:CS_2 = 1:1:3 at room temperature for 8 h. Notable, all the M_w values of the polymers were measured by GPC, and the traces were provided in supporting information (Figure S1).

After getting the optimal polymerization conditions, we further investigated the scope of activated alkynes by using them to react with diethyldithiocarbamic acid (Scheme 2). The experiments were conducted by first mixing diethylamine with CS_2 to form the diethyldithiocarbamic acid (**4**) intermediate, followed by the addition of alkynes to the reaction system. According to previous report,[41] phenylacetylene **5** can react with **4** to yield the sulfur-containing adduct **6** at 80 °C. However, a neat reaction was required as the use of solvent does not yield product. Notably, at room temperature, the carbonyl- or ester-activated internal alkynes **7** or **9** in solutions can spontaneously react with **4** to yield ADDC derivatives **8** and **10**, respectively. While, the most reactive carbonyl-activated terminal alkyne **11** would attract the diethylamine out from **4** to generate *β*-enaminone **12** via the spontaneous amino-yne click reaction.[21] It is worth noting that the binding ability of primary amines toward CS_2 is weaker than secondary aliphatic amines.[49] For example, in the presence of *n*-Bu_3P, primary amines can react with activated internal alkynes and CS_2 to produce a five-membered cyclic product (**15**).[50] However, the low yield and the presence of side products render it unsuitable for polymerization development.

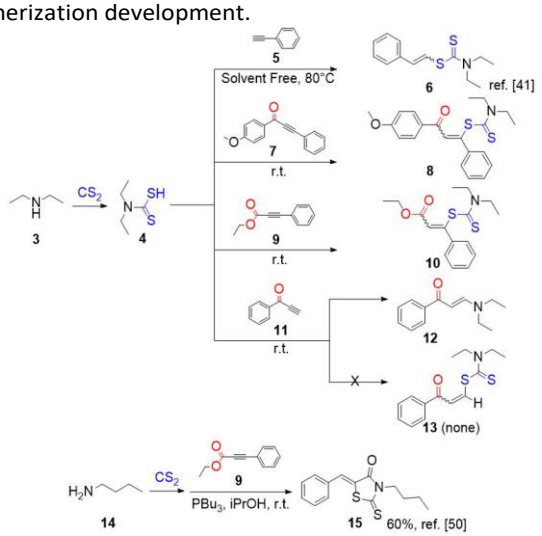

Scheme 2. Reaction of different alkynes with diethyldithiocarbamic acid (**4**).

Above results suggested that the carbonyl- or ester-activated internal alkyne precisely meet the demands for the spontaneous reaction with diethyldithiocarbamic acid. Therefore, we investigated the universality the polymerization of carbonyl- or ester-activated internal diyne and secondary aliphatic diamine monomers (Scheme 3 and Table 3). The results demonstrated that all the used diynes could readily polymerize with secondary diamines and CS_2 in a spontaneous manner, furnishing soluble polymers with high M_w (up to 31 600) and high yields (up to 97%). Notably, the polymerization carried out in air has less effect on the results compared with that under nitrogen, suggesting that moisture or oxygen did not significantly affect the efficiency of the spontaneous MCP.

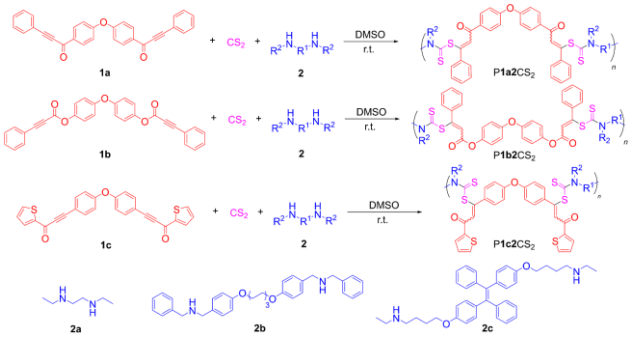

Scheme 3. Spontaneous multicomponent polymerization of activated internal diynes **1**, aliphatic secondary diamine **2** and CS_2.

Table 3. Spontaneous polymerizations of different activated internal diynes **1**, secondary amines **2**, and CS_2.[a]

entry	monomers	yield (%)	M_w [b]	$Đ$ [b]
1[c]	**1a**/**2a**/CS_2	75	21 700	1.94
2	**1a**/**2a**/CS_2	76	31 600	2.13
3	**1a**/**2b**/CS_2	92	21 200	1.81
4	**1a**/**2c**/CS_2	55	7100	1.39
5	**1b**/**2a**/CS_2	55	11 200	1.59
6	**1b**/**2b**/CS_2	80	14 900	1.67
7	**1c**/**2a**/CS_2	65	10 600	1.52
8	**1c**/**2b**/CS_2	97	31 400	1.93

[a] Carried out under nitrogen in anhydrous DMSO at 25 °C for 8 h, [CS_2] = 3[**1**] = 3[**2**] = 0.9 M. [b] Determined by gel-permeation chromatography (GPC) in DMF containing 0.05 M LiBr using linear PMMA for calibration. [c] Conducted under open air.

2.3 Structural Characterization

The resultant polymers generated by the spontaneous MCP were characterized using the Fourier transform infrared (FT-IR) and nuclear magnetic resonance (NMR) spectroscopy techniques. Herein, the characterization of P**1a2a**CS_2 was given as a representative example.

The FT-IR spectra of diyne **1a**, diamine **2a**, model compound **8**, and polymer P**1a2a**CS_2 are displayed in Figure 1. The spectra of **8** and P**1a2a**CS_2 are quite similar. The peak corresponding to the stretching vibration of the ethynyl group in **1a** appeared at 2195 cm^{-1}. This peak was almost absent in the spectrum of P**1a2a**CS_2, indicative of the consumption of diyne **1a** by the MCP. The remaining weak signal might be ascribed to the terminated

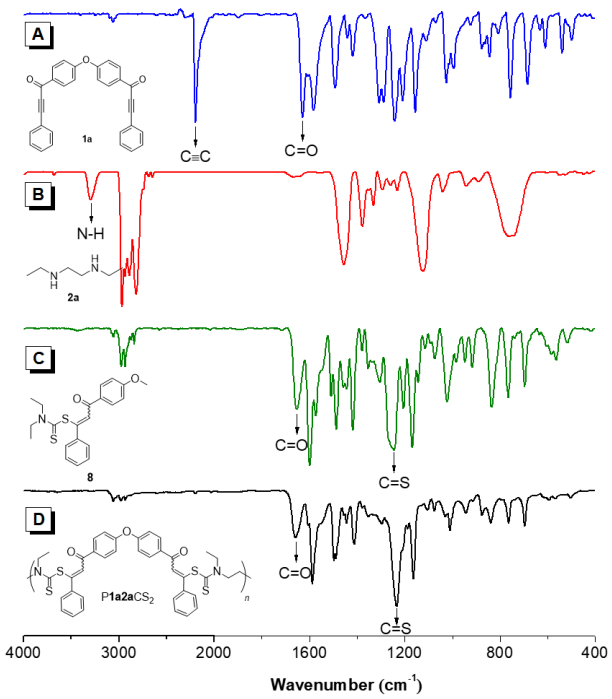

Figure 1. FT-IR spectra of (A) monomer **1a**, (B) monomer **2a**, (C) model compound **8**, and (D) polymer P**1a2a**CS_2.

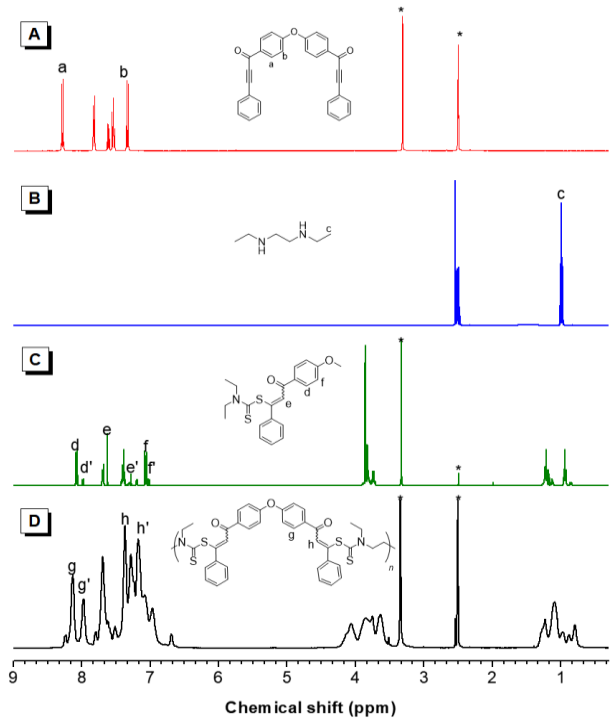

Figure 2. ^{1}H NMR spectra of (A) diyne **1a**, (B) diamine **2a**, (C) model compound **8**, and (D) polymer P**1a2a**CS_2 in DMSO-d_6. The solvent peaks are marked with asterisks.

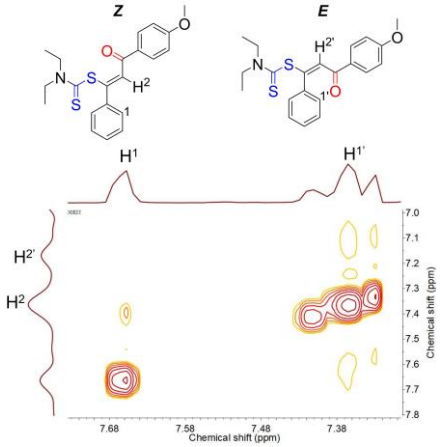

Figure 3. ^{1}H-^{1}H NOESY spectra of model compound **8** in $CDCl_3$.

ethynyl group of the polymer chains. Furthermore, the peaks corresponding to the C=S bond vibration in **8** and P**1a2a**CS_2 appeared at 1245 cm^{-1} and 1230 cm^{-1}, respectively.[51] Notably, neither *N*-H nor *S*-H peak was detected in compound **8** and P**1a2a**CS_2, and the positions of the other characteristic peaks were consistent with the structures of ADDC derivatives. These indicated that the MCP proceeded as expected. The FT-IR spectra of other polymers were similar to that of P**1a2a**CS_2 (Figure S2).

After having these clear picture of IR stretching peaks, we also monitored the polymerization process using *in situ* IR spectra analysis (Figure S3). When CS_2 was added to the mixture of **1a** and **2a** at 0 h, the intermediate dithiocarbamic acid was rapidly formed, resulting in an increase in the characteristic C-N peak at a wavenumber of 1519 cm^{-1}. Subsequently, the peak gradually decreased as the intermediate was consumed. The peak of C=O gradually shifted from 1635 cm^{-1} to 1661 cm^{-1}, indicative of the step-growth reaction of the intermediate with the activated diyne. Meanwhile, the generation of the C=C bond (1588 cm^{-1}) was also observed. These results demonstrated that the polymerization initially involved the rapid formation of dithiocarbamic acid intermediate from CS_2 and amines, followed by a gradual reaction with diyne monomers. The peaks showed a steady trend within 8 h, which is well consistent with the optimized reaction time.

^{1}H and ^{13}C NMR spectroscopy techniques were used to further confirm the structures of the polymers. The ^{1}H NMR spectra of **1a**, **2a**, **8**, and P**1a2a**CS_2 are shown in Figure 2 as an example. The proton resonance of vinyl group in **8** mainly appeared at 7.62 and 7.28 ppm due to the *E*/*Z*-isomers.[52,53] Since these two isomers are difficult to be separated by crystallization or column chromatography, they were then tested by ^{1}H-^{1}H nuclear overhauser effect spectroscopy (NOESY). As shown in Figure 3, a peak corresponding to the correlation between H^1 and H^2 was identified, while a prominent resonance related to the correlation between $H^{1'}$and $H^{2'}$ was not observed. This result indicated that H^2 is associated with the vinyl group in a *Z*-configuration and $H^{2'}$ represents the proton resonance of the vinyl group in an *E*-configuration. Therefore, the *E*/*Z* ratio of model compound **8** was calculated

from the integral areas as about 1:5, and *Z*-configuration was the dominant structure.

To exclude the possible hydroamination between the secondary amine and the alkyne, a control experiment was carried out by mixing compound **7** with diethylamine in THF, DCM, chloroform, or methanol. No product was found when the reaction was carried out at room temperature. Only when the mixture was heated to above 60 °C, *β*-enaminone derivative S**9** was detected and confirmed by NMR spectra (Figures S4 and S5). The proton resonance of vinyl group in S**9** at about 5.5- 6.0 ppm were not found in the ^{1}H NMR spectrum of model compound **8**, which rules out the possibility of a side reaction occurring between the secondary amine and **7**.

The ^{1}H NMR spectrum of P**1a2a**CS_2 is similar to model compound **8**, but with broad resonance peaks. The characteristic peak of the hydroamination product in the range of 5.5-6.0 ppm was also not observed. By comparing the polymer spectrum with **8**, we could find that both *E* and *Z*-units existed in P**1a2a**CS_2 with peaks at 7.37 and 7.17 ppm. The integral of H_g and H_g' indicated that *E*/*Z* ratio is 3:4.

The structure of the polymers could be further analyzed by ^{13}C NMR spectra (Figure 4). Two sets of the carbon resonant peaks were observed in the spectrum of **8**, attributed to the presence of *E* and *Z*-isomers. The peaks corresponding to the ethynyl carbons of **1a** appeared at 93.32 and 86.86 ppm. These peaks were absent in the spectra of **8** and P**1a2a**CS_2, proving the consumption of ethynyl groups by the reaction. Meanwhile, the carbon resonant peak of C=S unit appeared at 190 ppm. These characterization results demonstrated the successful synthesis of ADDC derivatives. The NMR spectra of the other monomers, polymers, and model compounds are presented in the Supporting Information (Figures S6-S11 and Figures S14-S27) and similar conclusions could be drawn.

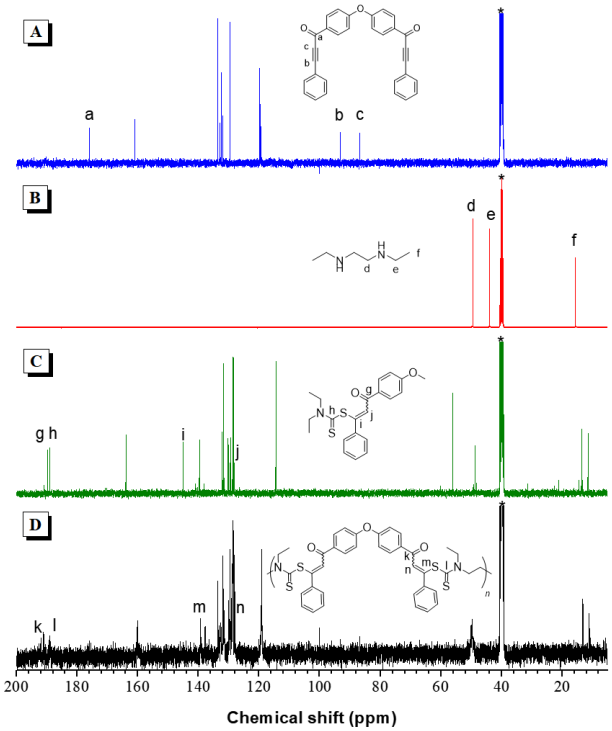

Figure 4. ^{13}C NMR spectra of (A) monomer **1a**, (B) monomer **2a**, (C) model compound **8**, and (D) polymer P**1a2a**CS_2 in DMSO-d_6. The solvent peaks are marked with asterisks.

2.4 Thermal Stability of Polymers

To study the thermal properties of PADDCs, thermogravimetric analysis (TGA) and differential scanning calorimetry (DSC) were conducted and the results are shown in Figure 5. As shown in Figure 5A, the temperatures (T_d) with 5% weight loss of polymers are all lower than 250 °C. This might be due to the containing dithiocarbamate groups that could be decomposed at elevated temperature. This property holds the potential to render polymers high-performance recyclable materials.[54] Interestingly, the T_d values of the polymers generated from **1b** are higher than those from **1a** and **1c**, suggesting that the electron-withdrawing groups in the polymer chains could impart remarkably effect on their thermal stability. In addition, the TGA curves of P**1a2a**CS_2 and P**1c2a**CS_2 displayed two decomposition stages. The first decomposition temperatures were approximately 175 °C, and the weight loss in this stage is corresponded to the loss of CS_2 content in the polymers. The second stage was not prominent and mainly corresponded to the degradation of other more stable units in polymers. The high char yields of P**1a2a**CS_2, P**1c2a**CS_2 and P**1c2b**CS_2 could be ascribed to their higher content of aromatic units than other polymers.

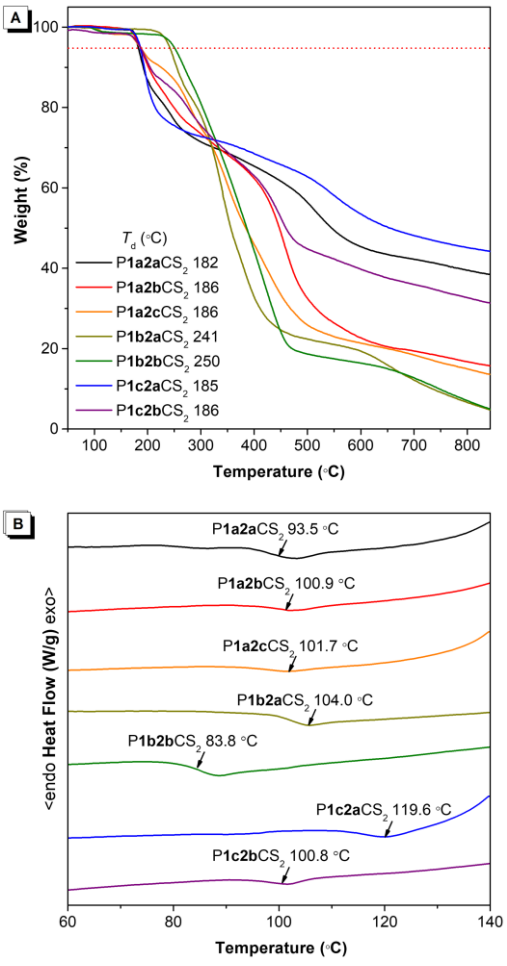

Figure 5. TGA thermograms (A) and DSC grams (B) of PADDCs under nitrogen.

The glass transition temperatures (T_g) of the polymers are in the range of 80-120 °C (Figure 5B). These temperatures are significantly lower than those of the initial decomposition,

ensuring that the polymers remain intact during thermo-processing. Interestingly, the subtle change of the comonomers during MCP led to distinct difference in the T_g values of polymers. For example, the polymers produced from **2a** generally have higher T_g values than the others except that its comonomer is **1a**. Although **2b** contains aromatic phenyl rings, it also has the flexible hexyl group, which resulted in a lower T_g values of the products. The higher T_g value of P**1a2a**CS_2 than that of P**1a2b**CS_2might be due to the chain packing of the former is better than the latter.

2.5 Light Transmittance of Polymers

The PADDCs contain a large amount of sulfur atoms, carbonyl groups, and aromatic groups, making them potentially useful as optical materials.[55,56] First, the light transmittances of polymer films, fabricated by spin-coating of their solutions with a concentration of 50 mg/mL, were measured using an ultraviolet-visible (UV-vis) spectrophotometer in the wavelength range of 300-900 nm. As shown in Figure 6, the light transmittance of most polymer films (except P**1c2a**CS_2) was higher than 85% beyond 400 nm, and the transmittances recorded for P**1b2a**CS_2 and P**1b2b**CS_2 films were as high as 90% at 400 nm. The transmittance decrease at the wavelength range of 300-500 nm might be caused by the absorption of polar chromophoric units in the polymers (Figure S12).

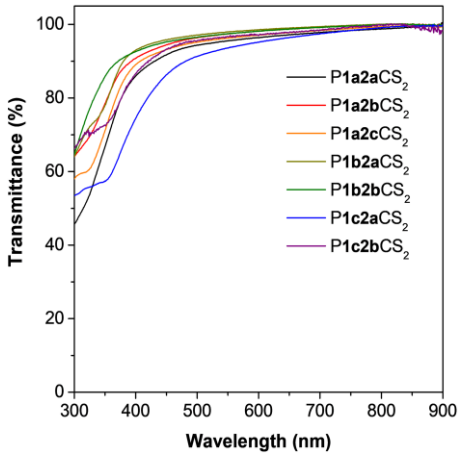

Figure 6. Light transmission spectra of the PADDCs films using quartz as basement.

2.6 Light Refraction Properties of Polymers

It is reported that the polymers contain polarizable aromatic rings and sulfur atoms might possess high refractive indices (*n*).[57,58] Thus, the *n* values of PADDCs were measured in the wavelength range of 400-1700 nm (Figure 7 and Table S3). The results showed that *n* values of the polymers at 632.8 nm are in the range of 1.65-1.75, which are significantly higher than that of commodity polymers, such as PMMA (n = 1.49) and polycarbonate (n = 1.59). Notably, the polymers generated from **1c**, characterized by a high sulfur content (F_S), showed outstanding *n* values. The highest *n* value of 1.7471 was recorded in P**1c2a**CS_2 with F_S value 27.7 w%. Meanwhile, the optical dispersion property shows a positive correlation with the *n* value. P**1a2b**CS_2 with the lowest *n* value among the resultant polymers possesses a low optical dispersion (*D*') of 0.004, which helps reduce the propagation loss of light. Thus, the excellent optical transmittance, high refractivity, and low dispersion demonstrate that PADDCs can potentially be used in the field of optical signal transmission.

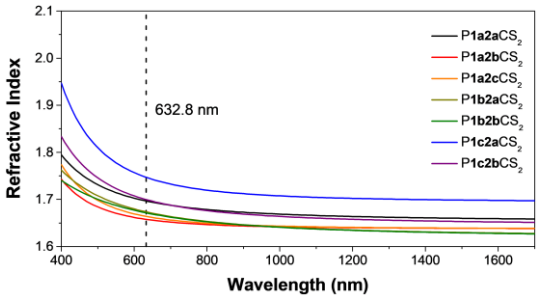

Figure 7. Wavelength dependence of refractive indices of the films of PADDCs using silica as basement.

2.7 Ultrathin Membranes of Polymers

It is reported that the surface tension, which is caused by the difference in surface free energy between water and polymer solutions, could drive the polymers to spread on the water surface as thin films.[59] Compared with spin coating and deposition techniques, the on-water spreading method is easier to fabricate large and thickness-controlled membranes, which could be used to fabricated optoelectronic devices by transfer printing of these membranes onto substrates.[60,61] Thanks to their excellent solubility in commonly used organic solvents, PADDCs could be easily spread to form high quality ultrathin membrane or fibers (Figure S13).

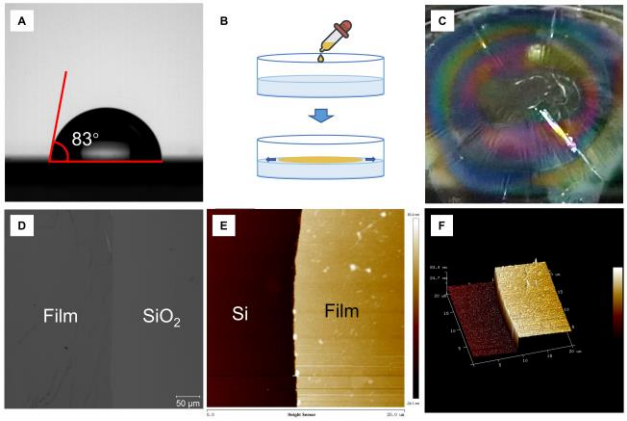

Figure 8. (A) Water contact angle of P**1a2a**CS_2 membrane on silica. (B) Preparation diagram of polymer membrane and (C) the large area membrane of P**1a2a**CS_2 spread on water. (D) Optical image of the ultrathin membrane on quartz fabricated using P**1a2a**CS_2 recorded by CLSM under bright field. (E) AFM image at the edge of the membrane on silica and its (F) three-dimensional image.

Experiments were conducted using P**1a2a**CS_2 as a representative example. The contact angle between the polymer membrane and water was measured to be 83° (Figure

8A). The specific surface free energy corresponding to P**1a2a**CS_2 was calculated to be approximately 33 J/m^2. It can be inferred that the surface tension is adequately high to result in the spontaneous spread of the polymer solution on water surface due to the higher free energy of water (72 J/m^2) (Figure 8B). As shown in Figure 8C, the large area ultrathin polymer membrane floating on water surface displays interference patterns under white light irradiation. The confocal laser scanning microscopy (CLSM) and atomic force microscopy (AFM) characterization of the membrane of P**1a2a**CS_2 (Figure 8D-F) suggest that the surface was smooth with a thickness of approximately 62.2 nm, and the average surface roughness (RA) was as low as 1.72 nm. The excellent film-forming properties of the polymers make them suitable for application in diverse fabrication.

Conclusions

In this work, we successfully developed a spontaneous multicomponent polymerization of activated internal diynes, secondary diamines and low-cost CS_2. Notably, the CS_2 acts like a "wedge" in "mortise and tenon" structure to connect the diynes and diamines in a spontaneous reaction manner, which generally required elevated temperature to occur. The regio-regular PADDCs with high M_w values (up to 31 600) were prepared at room temperature in high yields (up to 97%). The PADDCs possess good light transmittances and high refractive indices. In addition, the polymers are processible and could be fabricated into high quality ultrathin membrane by spreading method on water surface. The spontaneous MCP described in this study showcase green and sustainable characteristics, such as efficient CS_2 fixation, a straightforward reaction process, absence of toxic byproducts, and energy savings, and hold great potential to advance the utilization of sulfur-containing C1 monomers.

Conflicts of interest

There are no conflicts to declare.

Acknowledgements

This work was financially supported by the National Natural Science Foundation of China (21788102 and 21525417), the Natural Science Foundation of Guangdong Province (2019B030301003), and the Innovation and Technology Commission of Hong Kong (ITC-CNERC14SC01).

References

1 H. Mutlu, E. B. Ceper, X. Li, J. Yang, W. Dong, M. M. Ozmen, P. Theato, *Macromol. Rapid Commun.*, 2019, **40**, 1800650.
2 D. A. Boyd, *Angew. Chem. Int. Ed.*, 2016, **55**, 15486.
3 A. Kausar, S. Zulfiqar, M. I. Sarwar, *Polym. Rev.*, 2014, **54**, 185.
4 R.S. Glass, *Top. Curr. Chem.*, 2018, **376**, 22.
5 J. Zhang, Q. Zang, F. Yang, H. Zhang, J. Z. Sun, B. Z. Tang, *J. Am. Chem. Soc.*, 2021, **143**, 3944-3950.
6 A. S. Narmon, E. Leys, I. Khalil, G. Ivanushkin, M. Dusselier, *Green Chem.*, 2022, **24**, 9709.
7 T.-J. Yue, W.-M. Ren, L. Chen, G.-G. Gu, Y. Liu, X.-B. Lu, *Angew. Chem. Int. Ed.*, 2018, **57**, 12670.
8 K. F. Long, N. J. Bongiardina, P. Mayordomo, M. J.Olin, A. D. Ortega, C. N. Bowman, *Macromolecules*, 2020, **53**, 5805.
9 W. Cao, F. Dai, R. Hu, B. Z. Tang, *J. Am. Chem. Soc.*, 2020, **142**, 978.
10 M. Luo, Y. Li, Y. Y. Zhang, X. H. Zhang, *Polymer*, 2016, **82**, 406.
11 Y. Fan, H. Ben, L. Li, S. Meng, S. Zhang, X. Zheng, J. Zhang, L. Yin, S. Chen, *Appl. Catal., B* 2020, **274**, 119073.
12 J. L. Yang, Y. Wang, X. H. Cao, C. J. Zhang, Z. Chen, X. H. Zhang, *Macromol. Rapid Commun.*, 2021, **42**, e2000472.
13 B. Ochiai, T. Endo, *Prog. Polym. Sci.*, 2005, **30**, 183.
14 K. Nakano, G. Tatsumi, K. Nozaki, *J. Am. Chem. Soc.*, 2007, **129**, 15116.
15 M. Luo, X.-H. Zhang, D. J. Darensbourg, *Acc. Chem., Res.* 2016, **49**, 2209.
16 S. Wu, M. Luo, D. J. Darensbourg, X. Zuo, *Macromolecules*, 2019, **52**, 8596.
17 C. Zhao, X. Meng, R. Lu, H. Xie, J. Liu, *Polym. Chem.*, 2019, **10**, 5333.
18 X. Fu, A. Qin, B. Z. Tang, *Aggregate*, 2023, **4**, e350.
19 X. Chen, T. Bai, R. Hu, B. Song, L. Lu, J. Ling, A. Qin, B. Z. Tang, *Macromolecules*, 2020, **53**, 2516.
20 H. Kuroda, I. Tonita, T. Endo, *J. Polym. Sci., Part A: Polym. Chem.*, 1996, **34**, 1597.
21 S. Liu, J. Liu, Q. Wang, J. Wang, F. Huang, W. Wang, C. Sun, D. Chen, *Org. Chem. Front.*, 2020, **7**, 1137.
22 B. He, S. Zhen, Y. Wu, R. Hu, Z. Zhao, A. Qin, B. Z. Tang, *Polym. Chem.*, 2016, **7**, 7375.
23 R. Hu, B. Z. Tang, In *Multi-Component and Sequential Reactions in Polymer Synthesis,* Theato, P., Ed. Springer International Publishing: Cham, 2015, 17.
24 J. Wang, A. Qin, B. Z. Tang, *Macromol. Rapid Commun.*, 2021, **42**, 2000547.
25 X. Wang, B. Li, J. Peng, B. Wang, A. Qin, B. Z. Tang, *Macromolecules*, 2021, **54**, 6753.
26 Z. Zhang, Y. You, C. Hong, *Macromol. Rapid Commun.*, 2018, **39**, 1800362.
27 X. Wu, J. He, R. Hu, B. Z. Tang, *J. Am. Chem. Soc.*, 2021, **143**, 15723.
28 C. Wang, B. Yu, W. Li, W. Zou, H. Cong, Y. Shen, *Mater. Today Chem.*, 2022, **25**, 100948.
29 N. Zheng, H. Gao, Z. Jiang, W. Song, *Sci. China Chem.*, 2023, **66**, 870.
30 H. K. J. Hall, *Angew. Chem. Int. Ed.*, 1983, **22**, 440.
31 Q. Li, S. Ma, N. Lu, J. Qiu, J. Ye, Y. Liu, S. Wang, Y. Han, B. Wang, X. Xu, H. Feng, J. Zhu, *Green Chem.*, 2020, **22**, 7769.
32 P. A. J. M. de Jongh, D. M. Haddleton, K. Kempe, *Prog. Polym. Sci.*, 2018, **87**, 228.
33 X. Chen, R. Hu, C. Qi, X. Fu, J. Wang, B. He, D. Huang, A. Qin, B. Z. Tang, *Macromolecules*, 2019, **52**, 4526.
34 B. He, J. Zhang, J. Wang, Y. Wu, A. Qin, B. Z. Tang, *Macromolecules*, 2020, **53**, 5248.
35 L. Dong, W. Fu, P. Liu, J. Shi, B. Tong, Z. Cai, J. Zhi, Y. Dong, *Macromolecules*, 2020, **53**, 1054.
36 W. Fu, G. Zhu, J. Shi, B. Tong, Z. Cai, Y. Dong, *Chinese J. Polym. Sci.*, 2019, **37**, 981.
37 R. Hu, X. Chen, T. Zhou, H. Si, B. He, R. T. K. Kwok, A. Qin, B. Z. Tang, *Sci. China Chem.*, 2018, **62**, 1198.
38 O. S. Fenton, J. L. Andresen, M. Paolini, R. Langer, *Angew. Chem. Int. Ed.*, 2018, **57**, 16026.
39 Y. Liu, A. Qin, B. Z. Tang, *Prog. Polym. Sci.*, 2018, **78**, 92.
40 B. Song, D. Lu, A. Qin, B. Z. Tang, *J. Am. Chem. Soc.*, 2022, **144**, 1672.
41 F. Aryanasab, M. R. Saidi, *Monatsh. Chem.*, 2014, **145**, 521.
42 A. McClain, Y. L. Hsieh, *J. Appl. Polym. Sci.*, 2003, **92**, 218.
43 V. N. Elokhina, A. S. Nakhmanovich, A. E. Aleksandrova, B. I. Bishnevskii, I. D. Kalikhman, *Pharm. Chem. J.*, 1986, **20**, 1061.
44 J. Yan, Z. Chen, *Synth. Commun.*, 1999, **29**, 2867.
45 Y. Liu, W. Bao, *Tetrahedron Lett.*, 2007, **48**, 4785.

46 M. R. Wood, D. J. Duncalf, S. P. Rannard, Perrier, S. *Org. Lett.*, 2006, **8**, 553.
47 N. Azizi, F. Aryanasab, M. R. Saidi, *Org. Lett.*, 2006, **8**, 5275.
48 W.-F. Su, Step Polymerization. In: Principles of Polymer Design and Synthesis. Lecture Notes in Chemistry, Springer, Berlin, Heidelberg, 2013, **82**.
49 A. Z. Halimehjani, Y. L. Nosood, *Org. Lett.*, 2017, **19**, 6748.
50 S. Gabillet, D. Lecerclé, O. Loreau, M. Carboni, S. Dézard, J. M. Gomis, F. Taran, *Org. Lett.*, 2007, **9**, 3925.
51 Z. Chen, Y. Jin, P. J. Stang, *J. Org. Chem.*, 1987, **52**, 4117.
52 H. Deng, Z. He, J. W. Y. Lam, B. Z. Tang, *Polym. Chem.*, 2015, **6**, 8297.
53 M. Pramanik, K. Choudhuri, S. Chakraborty, A. Ghosh, P. Mal, *Chem. Commun.*, 2020, **56**, 2991.
54 Y. Wei, S. A. Hadigheh, *Compos. B Eng.*, 2023, **260**, 110786.
55 K. S. Kang, C. Olikagu, T. Lee, J. Bao, J. Molineux, L.N. Holmen, K. P. Martin, K. J. Kim, K. H. Kim, J. Bang. V. K. Kumirov, R. S. Glass, R. A. Norwood, J. T. Njardarson, J. Pyun, *J. Am. Chem. Soc.*, 2022, **144**(50), 23044.
56 M. Lee, Y. Oh, J. Yu, S. G. Jang, H. Yeo, J. J. Park, N. H. You, *Nat. Commun.*, 2023, **14**, 2866.
57 A. Nishant, K. -J. Kim, S. A. Showghi, R. Himmelhuber, T. S. Kleine, T. Lee, J. Pyun, R. A. Norwood, *Adv. Optical Mater.*, 2022, **10**, 2200176.
58 D. Xin, A. Qin, B. Z. Tang, *Polym. Chem.*, **2019**, *10*, 4271-4278.
59 H. Kuhn, *Thin Solid Films*, 1989, **178**, 1.
60 S. Tang, J. Gong, Y. Shi, S. Wen, Q. Zhao, *Nat. Commun.*, 2022, **13**, 3227.
61 S. Xiong, J. Li, J. Peng, X. Dong, F. Qin, W. Wang, L. Sun, Y. Xu, Q. Lin, Y. Zhou, *Adv. Opt. Mater.*, 2022, **10**, 2101837.

Supporting Information

Green Synthesis of Sulfur-Containing Polymers by Carbon Disulfide-based Spontaneous Multicomponent Polymerization

Xu Chen[a,b,d], Anjun Qin*[,a,b], Ben Zhong Tang*[,b,c,e]

[a]State Key Laboratory of Luminescent Materials and Devices, Guangdong Provincial Key Laboratory of Luminescence from Molecular Aggregates, South China University of Technology, Guangzhou 510640, China.

[b] Center for Aggregation-Induced Emission, AIE Institute, South China University of Technology, Guangzhou 510640, China

[c]School of Science and Engineering, Shenzhen Institute of Aggregate Science and Technology, The Chinese University of Hong Kong, Shenzhen (CUHK-Shenzhen), Guangdong 518172, China.

[d]Department of Infectious Diseases, the Fifth Affiliated Hospital, Sun Yat-sen University, 52 East Meihua Road, Zhuhai 519000, Guangdong Province, China.

[e]Hong Kong Branch of the Chinese National Engineering Research Centre for Tissue Restoration and Reconstruction, The Hong Kong University of Science & Technology, Kowloon 999077 Hong Kong, China.

Contents

Materials and Instruments

All experiments were carried out in a glove box or with the standard Schlenk techniques under dry nitrogen. Monomer 1,1'-(oxybis(4,1-phenylene))bis(3-phenylprop-2-yn-1-one) (**1a**), oxybis(4,1-phenylene)bis(3-phenylpropiolate) (**1b**), 3,3'-(oxybis(4,1-phenylene))bis(1-(thiophen-2-yl)prop-2-yn-1-one) (**1c**), 1,1'-((hexane-1,6-diylbis(oxy))-bis(4,1-phenylene))-bis(*N*-benzylmethanamine) (**2b**) and N-ethyl-4-(4-(2-(4-(3-(ethylamino)propoxy)phenyl)-1,2-diphenylvinyl) phenoxy)butan-1-amine (**2c**) were prepared following previously reported methods.[1-7] *N*,*N*'-Diethylethylenediamine (**2a**), ethyl phenylpropiolate (**9**) and CS_2 were purchased from TCI (Shanghai, China) Co. Ltd., and used without further purification. Anhydrous dimethyl sulfoxide (DMSO), *N*,*N*-dimethylformamide (DMF), and *N*,*N*-dimethylacetamide (DMAc) were purchased from Energy Chemical (Shanghai, China) and used directly. Tetrahydrofuran (THF) was distilled from sodium benzophenone ketyl under dry nitrogen before use. All other chemicals and reagents were commercially available and used as received without further purification. Water was purified with a Millipore filtration system.

^{1}H NMR and ^{13}C NMR spectra were measured on a Bruker AVANCE 400 (400 MHz) or AVANCE DRX 500 (500 MHz) NMR spectrometer (Bruker, Germany) using deuterated chloroform ($CDCl_3$) or deuterated dimethyl sulfoxide (DMSO-d_6) as solvent and tetramethyl silane (TMS, δ = 0) as internal reference. The weight-average molecular weights (M_w) and polydispersity indices ($Đ$ = M_w/M_n) of the polymers were measured by Waters 1515 gel permeation chromatography (GPC, Waters Associates, USA) system equipped with a RI detector. DMF containing 0.05 M LiBr was used as the eluent at a flow rate of 1.0 mL min^{-1}. A set of linear polymethyl methacrylate (PMMA) standards covering the M_w range of 10^3~10^7 were utilized for M_w and $Đ$ calibration. Fourier transform infrared (FT-IR) spectra were measured on a Vector 33 FT-IR (Bruker, Germany) spectrometer (KBr disk). Kinetic data analysis was obtained through in situ IR technique, and the polymerization spectra were recorded on a ReactIR 15 from Mettler Toledo AutoChem. Thermogravimetric analysis (TGA) was carried out on a TG 209 F3 (Netzsch, Germany) at a heating

rate of 20 °C/min in a nitrogen flow. The glass transition temperature (T_g) of polymers was characterized by differential scanning calorimetry (DSC 200 F3 Maia, NETZSCH, Germany) in nitrogen flow at a heating rate of 10 °C/min. The light transmittance and absorption were measured by UV-2600 spectrophotometer (Shimadzu, Japan). The polymer film samples were prepared by spinning the solution of polymers (50 mg/mL in dichlorobenzene) on quartz. Refractive index (n) curve was measured in air in the spectral range of 400-1700 nm by a V-VASE rotating analyzer ellipsometer (J. A. Woolam, USA). The polymer film samples were prepared by spinning the solution of polymers (50 mg/mL in dichlorobenzene) on plasma treated single-crystal silicon. The static water contact angle of polymer film on silica was measured by a sessile drop method using JC2000D1 (POWEREACH, Shanghai, China). The stretch curve of polymers was tested by electronic universal testing machine (Shimadzu AGS-X-50N, Japan). Confocal laser scanning microscopy (CLSM) (LSM 710, Zeiss, Germany) and scanning electron microscope (SEM) (Regulus8100, Hitachi, Japan) were used for morphological observation. The thickness of ultrathin membrane on silica were determined by a Innova atomic force microscopy (AFM) (Bruker, Germany).

Preparation of Monomer 1

Preparation of monomer **1a**

Monomer **1a** was synthetized according to the reported procedures.[1] The synthetic route is shown in Scheme **S1**.

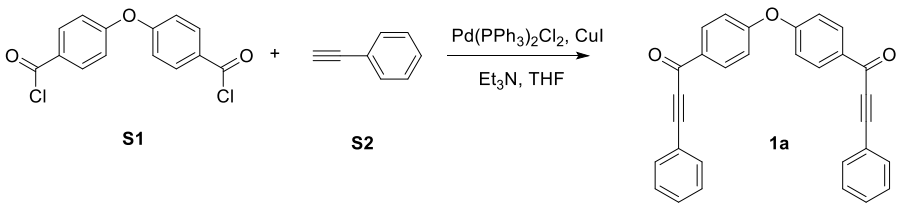

Scheme S1. Synthetic routes to monomer **1a**.

1,1'-(Oxybis(4,1-phenylene))bis(3-phenylprop-2-yn-1-one) (1a): Pd $(PPh_3)_2Cl_2$ (140 mg, 0.2 mmol), CuI (114 mg, 0.6 mmol), **S1** (2.95 g, 10 mmol), and distilled THF (100 mL) were added to a

250 mL two-necked round-bottom flask under nitrogen. Triethylamine (1.39 mL, 10 mmol) and phenylacetylene (**S2**, 2.84 mL, 25 mmol) were slowly injected into the solution. The mixture was stirred at room temperature for 6 h, and the formed precipitates were removed by filtration. After concentrated by a rotary evaporator under reduced pressure, the crude product was purified by a silica gel column chromatography using petroleum ether (PE)/ethyl acetate (EA) (10:1, *v*/*v*) as eluent. Off-white solid of **1a** was obtained in 77 % yield. ^{1}H NMR (400 MHz, DMSO-d_6), δ (TMS, ppm): 8.33 – 8.22 (m, 4H), 7.87 – 7.77 (m, 4H), 7.67 – 7.58 (m, 2H), 7.58 – 7.49 (m, 4H), 7.37 – 7.30 (m, 4H). ^{13}C NMR (100 MHz, DMSO-d_6), δ (TMS, ppm): 176.08, 161.06, 133.63, 132.91, 132.52, 132.01, 129.61, 119.80, 119.43, 93.32, 86.86. FT-IR (KBr disk), ν (cm^{-1}): 3061, 2195, 1628, 1582, 1493, 1418, 1307, 1289, 1242, 1207, 1156, 1025, 994, 877, 844, 756, 684, 609, 539, 498.

Preparation of monomer **1b**

Monomer **1b** was synthetized according to the reported procedures,[2,3] and the synthetic route is shown in Scheme **S2**.

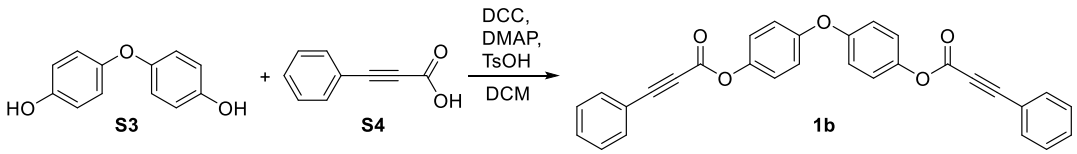

Scheme S2. Synthetic routes to monomer **1b**.

Oxybis(4,1-phenylene) bis(3-phenylpropiolate) (1b): **S3** (10 mmol, 2.02 g), *N*,*N*'-dicyclohexylcarbodiimide (DCC, 30 mmol, 6.19 g), 4-dimethylaminopyridine (DMAP, 4 mmol, 489 mg) and 4-methylbenzenesulfonic acid (TsOH, 4 mmol, 689 mg) were added into a 250 mL two-necked round bottom flask. The flask was evacuated under vacuum and flushed with dry nitrogen for three times and 80 mL dichloromethane (DCM) was added. Then **S4** (30 mmol, 4.38 g) in 20 mL DCM was injected into the system dropwise. After finishing the addition, the mixture was stirred at room temperature overnight. Afterward, the solvent was evaporated and the crude product was purified by a silica gel column chromatography using PE/EA (10:1 *v*/*v*) as eluent. White solid of **1b** was obtained in 98% yield. ^{1}H NMR (500 MHz, $CDCl_3$), δ (TMS, ppm): 7.64 (d, J = 7.2 Hz, 4H),

7.49 (t, *J* = 7.5 Hz, 2H), 7.41 (t, *J* = 7.6 Hz, 4H), 7.17 (d, *J* = 8.9 Hz, 4H), 7.05 (d, *J* = 9.0 Hz, 4H). ^{13}C NMR (125 MHz, $CDCl_3$), δ (TMS, ppm): 155.04, 152.45, 145.70, 133.20, 131.10, 128.70, 122.78, 119.70, 119.21, 88.90, 80.16. FT-IR (KBr disk), ν (cm^{-1}): 3106, 3065, 2232, 1721, 1594, 1491, 1444, 1284, 1250, 1183, 1146, 1099, 1006, 947, 925, 857, 760, 734, 687, 614, 587, 534, 512.

Preparation of monomer **1c**

Monomer **1c** was synthetized in similar procedure as **1a**.[4] The synthetic routes are shown in Scheme **S3**.

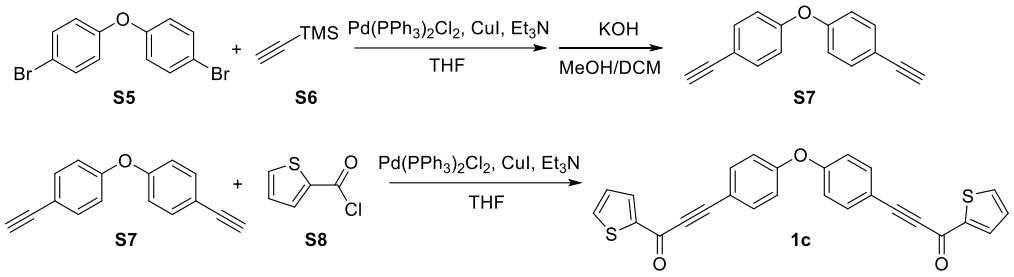

Scheme S3. Synthetic routes to monomer **1c**.

4,4'-Oxybis(ethynylbenzene) (S7): $PdCl_2(PPh_3)_2$ (701.9 mg, 1 mmol), CuI (380.9 mg, 2 mmol), **S5** (3.28 g, 10 mmol) were added into a 250 mL two-necked round bottom flask, and dissolved with 60 mL triethylamine and 10 mL distilled THF under nitrogen. After addition of trimethylsilylacetylene (**S6**, 5.65 mL, 40 mmol), the mixture was refluxed for 12 h. After evaporating the solvent and purified by silica gel column chromatography using petroleum as eluent, white solid of TMS protected product was obtained. The above solid was dissolved together with KOH (3.366 g, 60 mmol) in DCM and methanol, and stirred at room temperature for 4 h. A white solid of **S7** can be obtained after purification by silica gel column chromatography using PE as eluent (yield 83%). ^{1}H NMR (500 MHz, $CDCl_3$), δ (TMS, ppm): 7.47 (d, *J* = 8.8 Hz, 4H), 6.95 (d, *J* = 8.8 Hz, 4H), 3.05 (s, 2H). ^{13}C NMR (125 MHz, $CDCl_3$), δ (TMS, ppm): 157.04, 133.90, 118.89, 117.37, 83.04.

3,3'-(Oxybis(4,1-phenylene))bis(1-(thiophen-2-yl)prop-2-yn-1-one) (1c): $PdCl_2(PPh_3)_2$ (7 mg, 0.01 mmol), CuI (3.8 mg, 0.02 mmol), **S7** (109 mg, 0.5 mmol), and distilled THF (10 mL) were added into a 50 mL two-necked round-bottom flask under nitrogen. Then triethylamine (173 μL, 1.25 mmol)

and **S8** (134 μL, 1.25 mmol) was injected into the solution. The mixture was stirred at room temperature for 6 h. After reaction, the precipitates were removed by filtration, and the solution was concentrated by a rotary evaporator under reduced pressure to get the crude product, which can be purified by a silica gel column chromatography using PE/EA (10:1, *v*/*v*) as eluent. 177 mg off-white solid of was obtained in 81% yield. ^{1}H NMR (500 MHz, $CDCl_3$), δ (TMS, ppm): 8.01 (m, 2H), 7.74 (m, 2H), 7.69 (d, J = 8.8 Hz, 4H), 7.20 (m, 2H), 7.08 (d, J = 8.8 Hz, 2H). ^{13}C NMR (125 MHz, $CDCl_3$), δ (TMS, ppm): 169.70, 158.36, 144.94, 135.26, 135.25, 134.97, 128.37, 119.36, 115.45, 91.22, 86.70. FT-IR (KBr disk), v (cm^{-1}): 3054, 2937, 2870, 2813, 1604, 1572, 1507, 1473, 1446, 1386, 1586, 1243, 1176, 1132, 1113, 1052, 1028, 972, 820, 743, 700, 612, 573, 512.

Preparation of Monomers 2

Preparation of monomer **2b**

Monomer **2b** was synthetized according to the method reported before.[5,6]

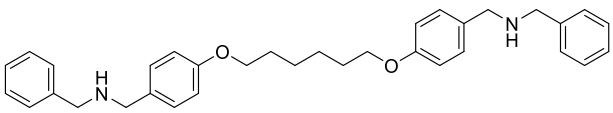

2b

1,1'-((Hexane-1,6-diylbis(oxy))-bis(4,1-phenylene))-bis(*N*-benzylmethanamine) (2b): White solid in 87% yield. ^{1}H NMR (500 MHz, $CDCl_3$), δ (TMS, ppm): 7.33 (m, 8H), 7.24 (m, 6H), 6.86 (d, J = 8.7 Hz, 4H), 3.96 (t, J = 6.8Hz, 4H), 3.79 (s, 4H), 3.74 (s, 4H), 1.81 (m, 4H), 1.61 (s, 2H), 1.54 (m, 4H). ^{13}C NMR (125 MHz, $CDCl_3$), δ (TMS, ppm): 158.14, 140.39, 132.30, 129.30, 128.37, 128.15, 126.89, 114.39, 67.84, 53.06, 52.58, 29.25, 25.89. FT-IR (KBr disk), v (cm^{-1}): 3341, 3058, 3026, 2938, 2868, 2821, 1609, 1581, 1510, 1474, 1448, 1289, 1250, 1165, 1105, 1025, 824, 730, 697, 609, 513.

Preparation of monomer **2c**

Monomer **2c** was synthesized according to the reported method.[5,7]

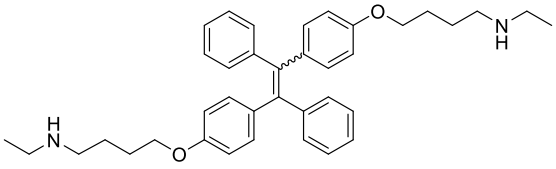

2c

N-ethyl-4-(4-(2-(4-(3-(ethylamino)propoxy)phenyl)-1,2-diphenylvinyl)phenoxy)butan-1-amine (2c): Yellow-green viscous product in 89% yield. ^{1}H NMR (500 MHz, $CDCl_3$), δ (TMS, ppm): 7.13 – 6.97 (m, 10H), 6.96 – 6.82 (m, 4H), 6.66 – 6.54 (m, 4H), 3.87 (t, J = 6.3 Hz, 4H), 2.76 – 2.60 (m, 8H), 1.84 – 1.72 (m, 4H), 1.66 (m, 4H), 1.13 (t, J = 7.2 Hz, 6H). ^{13}C NMR (125 MHz, $CDCl_3$), δ (TMS, ppm): 157.33, 144.29, 139.59, 136.25, 132.49, 131.35, 127.62, 126.11, 113.48, 67.40, 49.25, 43.96, 27.08, 26.40, 26.39, 14.93, 14.92. FT-IR (KBr disk), ν (cm^{-1}): 3054, 2937, 2870, 2813, 1604, 1572, 1507, 1473, 1446, 1386, 1586, 1243, 1176, 1132, 1113, 1052, 1028, 972, 820, 743, 700, 612, 573, 512.

Model Reactions

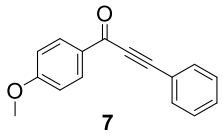

7

1-(4-Methoxyphenyl)-3-phenylprop-2-yn-1-one (7): compound **7** was synthetized in a similar procedure as **1a** to obtain white solid in 86% yield. ^{1}H NMR (400 MHz, $CDCl_3$), δ (TMS, ppm): 8.26 – 8.16 (m, 2H), 7.72 – 7.64 (m, 2H), 7.52 – 7.37 (m, 3H), 7.04 – 6.94 (m, 2H), 3.90 (s, 3H). ^{13}C NMR (100 MHz, $CDCl_3$), δ (TMS, ppm): 176.71, 164.51, 132.98, 132.01, 130.60, 130.36, 128.67, 120.40, 113.91, 92.34, 86.95, 55.62.

In order to verify the structure of the intermediate produced by secondary amines with CS_2, diethyldithiocarbamic acid (**4**) was prepared according to the route shown in Scheme S4:

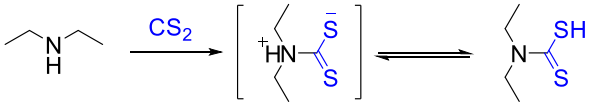

3 **4**

Scheme S4. Synthetic route to intermediate **4**.

After slowly mixed diethylamine (515 μL, 5 mmol) with excess CS_2 (604 μL, 10 mmol), the system began to release heat and finished after 10 min. By removing the remaining CS_2 with rotary evaporation, the colorless crystal of compound **4** was obtained equivalently. The compound was unstable and needed to be stored at low temperature under nitrogen atmosphere. ^{1}H NMR (400 MHz, $CDCl_3$), δ (TMS, ppm): 8.57 (s, 1H), 4.10 (q, J = 7.0 Hz, 2H), 3.16 (q, J = 7.3 Hz, 2H), 1.38 (t, J = 7.3 Hz, 3H), 1.26 (t, J = 7.0 Hz, 3H). ^{13}C NMR (100 MHz, $CDCl_3$), δ (TMS, ppm): 208.68, 47.88, 40.79, 12.39, 11.10.

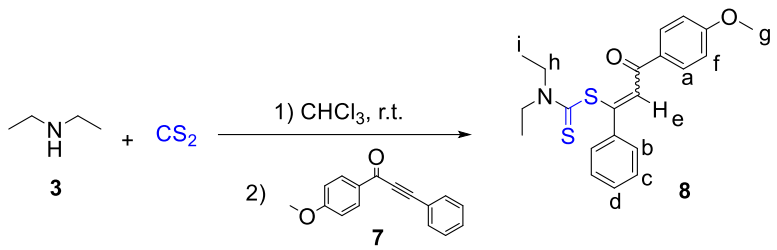

Scheme S5. Synthetic route to model compound **8**.

3-(4-Methoxyphenyl)-3-oxo-1-phenylprop-1-en-1-yl diethyldithiocarbamic acid (8): Model compound **8** was prepared in a similar procedure as the literature (Scheme S5).[8] Diethylamine (15.5 μL, 0.15 mmol) was dissolved with 0.2 mL chloroform in a 25 mL Schleck tube, then CS_2 (27.2 μL, 0.45 mmol) was added and heat release can be observed. The mixture was stirred until it recovered to room temperature, then compound **7** (35.4 mg, 0.15 mmol) dissolved in 0.2 mL chloroform was injected. Subsequently, the wall of the tube was washed with another 0.1 mL of chloroform. The reaction was conducted at room temperature for 8 h. Following the completion of the reaction, the organic solvent was removed by rotary evaporator. The product was purified by silica gel column using PE/EA (10:1 *v*/*v*) as eluent. Compound **8** was obtained in 86% yield as a yellow oil. ^{1}H NMR (400 MHz, DMSO-d_6), δ (TMS, ppm): 8.11 – 8.04 (d, *Z*-H_a), 7.98 (d, *E*-$H_{a'}$), 7.72 – 7.66 (m, *Z*-H_c), 7.62 (s, *Z*-H_e), 7.43 – 7.36 (m, *Z*-H_b, H_d), 7.33 – 7.29 (m, *E*-$H_{c'}$), 7.28 (s, *E*-$H_{e'}$), 7.22 – 7.17 (m, *E*-$H_{b'}$, $H_{d'}$), 7.10 – 7.04 (d, *Z*-H_f), 7.02 (d, *E*-$H_{f'}$), 3.86 (s, *Z*-H_g), 3.84 – 3.78 (m, *E*-$H_{g'}$, $H_{h'}$), 3.74 (q, *Z*-H_h), 0.94 (t, *Z*-H_i), 0.85 (m, *E*-$H_{i'}$). ^{13}C NMR (100 MHz, DMSO-d_6), δ (TMS, ppm): 190.97, 189.90,

189.13, 164.05, 163.93, 145.07, 141.09, 139.86, 139.72, 138.24, 132.19, 131.84, 131.65, 130.25, 129.74, 129.35, 128.87, 128.68, 128.44, 128.09, 114.58, 114.51, 56.09, 49.30, 48.77, 48.67, 48.23, 31.43, 22.54, 14.56, 13.64, 13.40, 11.73, 11.40. FT-IR (KBr disk), ν (cm^{-1}): 3056, 2974, 2932, 2838, 1652, 1598, 1487, 1458, 1444, 1418, 1304, 1245, 1205, 1168, 1073, 1022, 947, 915, 834, 766, 696, 563, 517.

Model compound **S9** was prepared to compare with model compound **8**, and prove that there is no by-product of direct amino-yne reaction in the multicomponent reaction of this work. The synthetic routes to compound **S9** are show in Scheme **S6**:

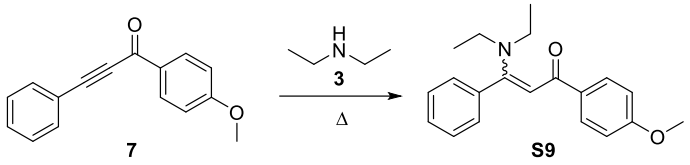

Scheme S6. Synthetic routes to model compound **S9**.

3-(Diethylamino)-1-(4-methoxyphenyl)-3-phenylprop-2-en-1-one (S9): Compound **7** (35.4 mg, 0.15 mmol) was dissolved in 2 mL methanol, then diethyl amine (20.6 μL, 0.2 mmol) was added. The mixture was heat to 60 ℃ for 8 h. The product was obtained by solvent evaporation and purification by a silica gel column using PE/EA (10:1, *v*/*v*) as eluent. Yellow oily liquid of **S9** was obtained in 96% yield. ^{1}H NMR (500 MHz, $CDCl_3$), δ (TMS, ppm): 7.89 (d, J = 8.8 Hz, 0.08H), 7.83 (d, J = 8.8 Hz, 1.92H), 7.51 – 7.33 (m, 3H), 7.28 – 7.17 (m, 2H), 6.84 (d, J = 8.9 Hz, 2H), 5.94 (s, *Z*-C=CH-S, 0.96H), 5.67 (s, *E*-C=CH-S, 0.04H), 3.80 (s, 3H), 3.26 (s, 4H), 1.18 (s, 6H). ^{13}C NMR (125 MHz, $CDCl_3$), δ (TMS, ppm): 186.07, 162.73, 161.53, 137.39, 134.78, 129.45, 128.40, 128.09, 127.82, 113.04, 92.92, 55.28, 44.16, 13.38.

Model compound **10** was prepared in similar procedure as compound **8** (Scheme S7):

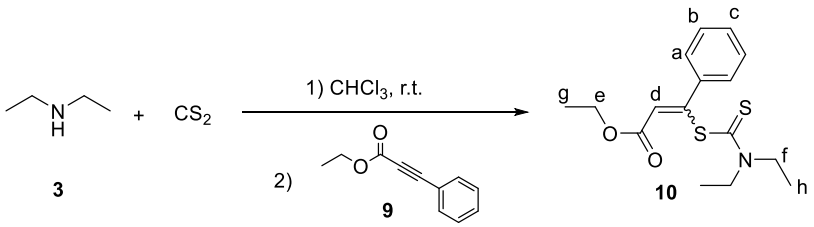

Scheme S7. Synthetic route to model compound **10**.

Ethyl 3-((diethylcarbamothioyl)thio)-3-phenylacrylate (10): Yellow oil, yield 91%. ^{1}H NMR (500 MHz, $CDCl_3$), δ (TMS, ppm): 7.63 – 7.56 (m, *Z*-H_a), 7.51 – 7.45 (m, *E*-$H_{a'}$), 7.38 – 7.32 (m, *Z*-H_b, H_c), 7.32 – 7.28 (m, *E*-$H_{b'}$, $H_{c'}$), 6.55 (s, *Z*-H_d), 6.47 (s, *E*-$H_{d'}$), 4.23 (q, *Z*-H_e), 4.06 (q, *E*-$H_{e'}$), 3.89 (m, *Z*-H_f), 3.78 (m, *E*-$H_{f'}$), 1.42 – 1.35 (m, *Z*-H_g), 1.34 – 1.25 (m, *Z*-H_h), 1.20 – 1.06 (m, *E*-$H_{g'}$, $H_{h'}$). ^{13}C NMR (125 MHz, $CDCl_3$), δ (TMS, ppm): 190.71, 190.12, 164.68, 164.53, 149.22, 149.14, 139.85, 137.20, 130.04, 129.29, 128.83, 128.34, 128.24, 127.83, 127.18, 125.20, 60.63, 60.52, 49.01, 48.84, 48.51, 48.11, 14.26, 13.92, 13.38, 13.22, 11.38, 11.32.

Typical Procedures for Polymerization

Without additional notes, all the polymerizations were performed under nitrogen atmosphere following standard Schlenk technique. A representative process for the polymerization of P**1a2a**CS_2 is presented in the following section.

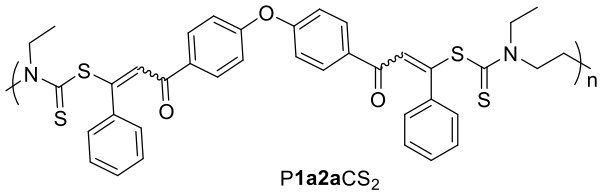

P**1a2a**CS_2

P**1a2a**CS_2. Monomer **2a** (21.5 μL, 0.15 mmol) in 0.2 mL DMSO was firstly added into a 25 mL Schleck tube and mixed with CS_2 (27.2 μL, 0.45 mmol). After a heat release process, monomer **1a** (63.9 mg, 0.15 mmol) dissolved in 0.2 mL DMSO was injected, and then the wall of tube was washed with another 0.1 mL of DMSO. The reaction was conducted at room temperature for 8 h, then quenched with 20 mL water. The reaction mixture was extracted thrice with saturated brine and DCM. The organic phase was dried with anhydrous sodium. The polymer was precipitated by adding the solution dropwise into 125 mL of hexane under vigorous stirring. The precipitates were filtered, washed with hexane, and dried in vacuum at 40 ℃ to a constant weight. The product was obtained as a yellow solid in 76% yield. M_w: 31 600, $Đ$: 2.13. FT-IR (KBr disk), ν (cm^{-1}): 3055, 2976, 2930,

1657, 1587, 1497, 1443, 1411, 1233, 1163, 1009, 942, 875, 838, 763, 695. ^{1}H NMR (400 MHz, DMSO-d_6), δ (TMS, ppm): 8.13 (s, 2.3H), 7.97 (s, 1.7H), 7.69 (s, 4H), 7.47 – 6.62 (m, 12H), 3.83 (m, 8H), 1.42 – 0.57 (m, 6H). ^{13}C NMR (100 MHz, DMSO-d_6), δ (TMS, ppm): 191.87, 191.22, 189.21, 188.84, 160.23, 160.15, 139.43, 139.13, 137.86, 133.60, 133.18, 132.75, 132.48, 131.95, 131.55, 130.08, 129.57, 129.07, 128.75, 128.61, 128.08, 119.44, 119.25, 100.00, 50.25, 49.73, 13.29, 13.12, 11.23, 10.86.

Optimization of Polymerization Conditions

Table S1. Effect of CS_2 amount on the spontaneous polymerization of **1a**, **2a** and CS_2.[a]

entry	equivalent of CS_2 (eq)	yield (%)	M_w [b]	$Đ$ [b]
1	2	73	25 600	1.83
2	3	74	28 300	1.99
3	4	74	25 300	1.89

[a] Carried out under nitrogen in anhydrous DMSO at 25 °C, [**1a**] = [**2a**] = 0.3 M. [b] Determined by GPC in DMF containing 0.05 M LiBr using linear PMMA for calibration.

Table S2. Time course of the spontaneous polymerization of **1a**, **2a** and CS_2.[a]

entry	time (h)	yield (%)	M_w [b]	$Đ$ [b]
1	1	56	14 000	1.84
2	2	67	15 100	1.79
3	4	76	19 400	1.82
4	8	76	31 600	2.13
5	12	75	28 100	1.93

[a] Carried out under nitrogen in anhydrous DMSO at 25 °C, [**1a**] = [**2a**] = 0.3 M, [CS_2] = 0.9 M. [b] Determined by GPC in DMF containing 0.05 M LiBr using linear PMMA for calibration.

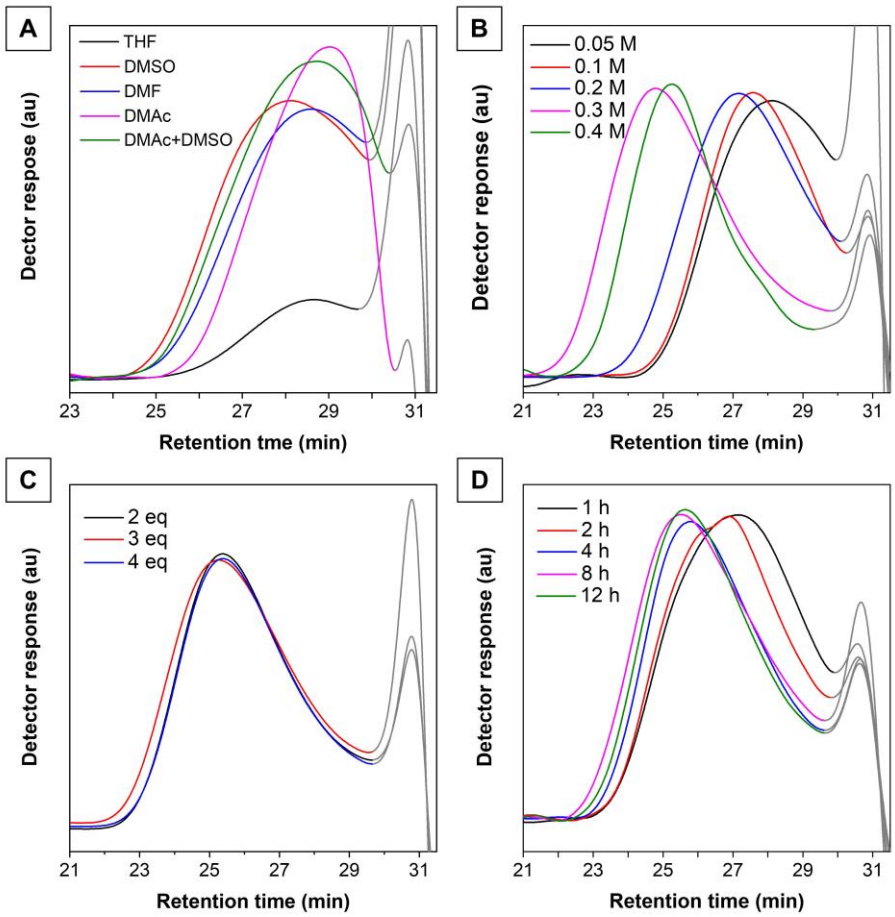

Figure S1. GPC traces of the products during polymerization condition optimization. (A) GPC traces of P**1a2a**CS_2 prepared in different solvent. (B) GPC traces of P**1a2a**CS_2 prepared under different concentration. (C) GPC traces of P**1a2a**CS_2 prepared with different CS_2 equivalent. (D) GPC traces of P**1a2a**CS_2 at different time intervals. The gray part is the peaks caused by the solvent.

Characterization Data for PADDCs

The other polymers were prepared according to the method similar to that of P**1a2a**CS_2. The characterization data of the polymer are as follows:

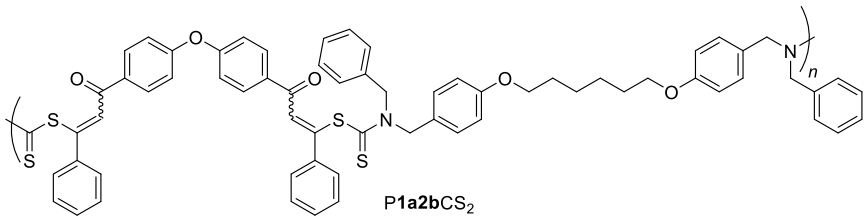

P**1a2b**CS_2

P**1a2b**CS_2. The polymer was obtained as a yellow solid in 92% yield. M_w: 21 200, $Đ$: 1.81. FT-IR (KBr disk), ν (cm^{-1}): 3058, 3031, 3935, 2862, 1658, 1608, 1585, 1511, 1495, 1470, 1407, 1351, 1303, 1235, 1612, 1111, 1076, 1028, 1011, 968, 942, 874, 838, 762, 734, 696, 593. ^{1}H NMR (400 MHz,

DMSO-d_6), δ (TMS, ppm): 8.15 (s, 2H), 7.94 (s, 2H), 7.67 (d, 4H), 7.47 – 6.68 (m, 30H), 5.28 – 4.84 (m, 8H), 3.91 (d, 4H), 1.68 (s, 4H), 1.34 (s, 4H). ^{13}C NMR (100 MHz, DMSO-d_6), δ (TMS, ppm): 194.00, 193.69, 191.11, 189.14, 160.25, 158.81, 139.50, 137.69, 135.55, 131.98, 130.21, 129.31, 128.87, 128.81, 128.06, 127.66, 127.22, 119.30, 115.22, 114.78, 67.90, 56.17, 55.94, 29.08, 25.78.

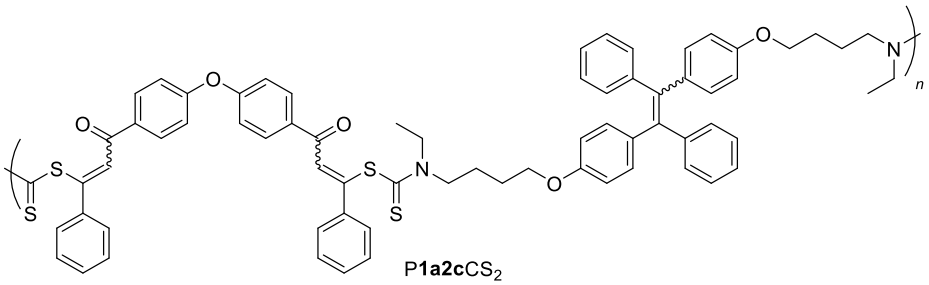

P**1a2c**CS_2

P**1a2c**CS_2. The polymer was obtained as a yellow solid in 55% yield. M_w: 7100, $Đ$: 1.39. FT-IR (KBr disk), v (cm^{-1}): 3055, 2934, 2870, 2197, 1656, 1605, 1587, 1507, 1491, 1443, 1416, 1374, 1239, 1163, 1071, 1029, 1009, 874, 835, 761, 700, 612, 569. ^{1}H NMR (400 MHz, DMSO-d_6), δ (TMS, ppm): 8.03 (d, 4H), 7.61 (d, 4H), 7.41 – 6.52 (m, 32H), 3.99 – 3.59 (m, 12H), 1.59 (d, 6H), 1.21 (d, 4H), 0.86 (t, 6H). ^{13}C NMR (100 MHz, DMSO-d_6), δ (TMS, ppm): 190.25, 190.08, 189.02, 160.16, 157.42, 144.18, 139.71, 136.10, 133.60, 133.25, 132.37, 131.88, 131.22, 129.97, 129.56, 128.67, 128.50, 128.12, 126.70, 119.22, 114.18, 67.38, 53.60, 49.00, 31.44, 26.30, 25.07, 23.04, 22.55, 14.45, 13.62, 11.28.

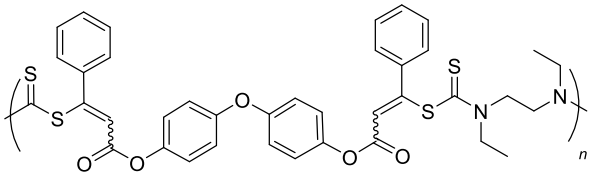

P**1b2a**CS_2

P**1b2a**CS_2. The polymer was obtained as a white solid in 55% yield. M_w: 11 200, $Đ$: 1.59. FT-IR (KBr disk), v (cm^{-1}): 3056, 2978, 2931, 1735, 1594, 1571, 1491, 1444, 1413, 1353, 1300, 1242, 1185, 1126, 1011, 989, 897, 847, 764, 696, 516. ^{1}H NMR (400 MHz, DMSO-d_6), δ (TMS, ppm): 7.65 (d, 4H), 7.55 – 6.88 (m, 14H), 6.51 (d, 2H), 4.29 – 3.56 (m, 8H), 1.36 – 0.77 (m, 6H). ^{13}C NMR (100 MHz, DMSO-d_6), δ (TMS, ppm): 188.72, 163.44, 162.61, 154.80, 154.53, 146.23, 138.40, 136.30, 133.50, 130.27, 129.67, 129.20, 128.98, 128.67, 128.32, 128.16, 123.71, 123.48, 119.97, 119.83, 54.32, 52.20,

50.10, 13.21, 11.55, 11.05. 155.04, 152.45, 145.70, 133.20, 131.10, 128.70, 122.78, 119.70, 119.21, 88.90, 80.16.

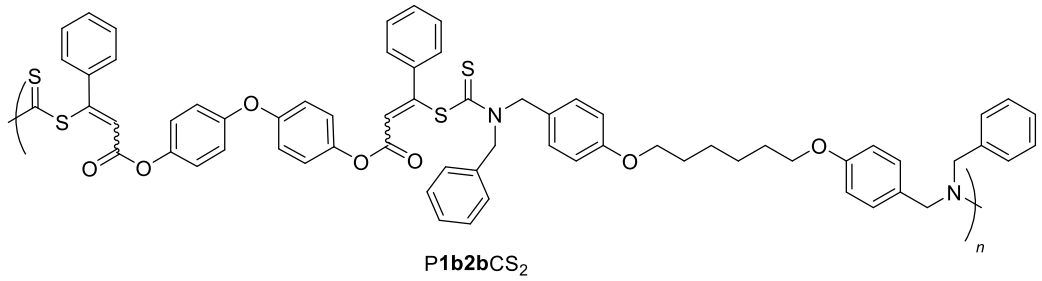

P**1b2b**CS_2

P**1b2b**CS_2. The polymer was obtained as a white solid in 80% yield. M_w: 14 900, $Đ$: 1.67. FT-IR (KBr disk), v (cm^{-1}): 3059, 2937, 2864, 1733, 1608, 1511, 1491, 1470, 1408, 1351, 1301, 1247, 1182, 1126, 1012, 964, 847, 764, 734, 696, 517. ^{1}H NMR (400 MHz, DMSO-d_6), δ (TMS, ppm): 7.76 – 6.63 (m, 38H), 5.06 (s, 8H), 3.89 (s, 4H), 1.67 (s, 4H), 1.41 (s, 4H). ^{13}C NMR (100 MHz, DMSO-d_6), δ (TMS, ppm): 193.47, 193.28, 163.20, 158.81, 158.63, 154.73, 150.53, 146.26, 139.13, 135.59, 133.48, 130.64, 130.32, 129.65, 129.46, 129.35, 128.99, 128.91, 128.88, 128.78, 128.23, 127.88, 127.71, 127.63, 127.24, 124.60, 123.70, 123.47, 119.88, 119.79, 115.24, 114.79, 67.82, 56.38, 29.08, 25.78.

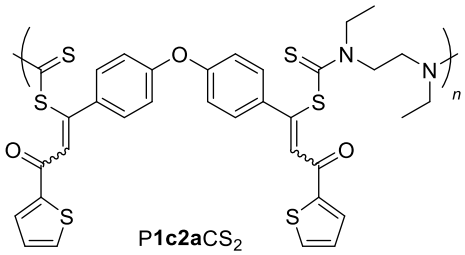

P**1c2a**CS_2

P**1c2a**CS_2. The polymer was obtained as a yellow solid in 65% yield. M_w: 10 600, $Đ$: 1.52. FT-IR (KBr disk), v (cm^{-1}): 3091, 2977, 2930, 2194, 1635, 1589, 1492, 1411, 1354, 1237, 1167, 1079, 1058, 1011, 927, 857, 831, 724. ^{1}H NMR (400 MHz, DMSO-d_6), δ (TMS, ppm): 8.02 (m, 4H), 7.78 – 7.47 (m, 4H), 7.47 – 6.63 (m, 8H), 4.30 – 3.57 (m, 8H), 1.40 – 0.72(m, 6H). ^{13}C NMR (100 MHz, DMSO-d_6), δ (TMS, ppm): 188.71, 181.96, 181.26, 157.61, 156.91, 145.43, 145.30, 136.27, 135.00, 134.42, 132.29, 130.86, 129.37, 118.77, 50.47, 49.73, 13.38, 13.24, 10.91.

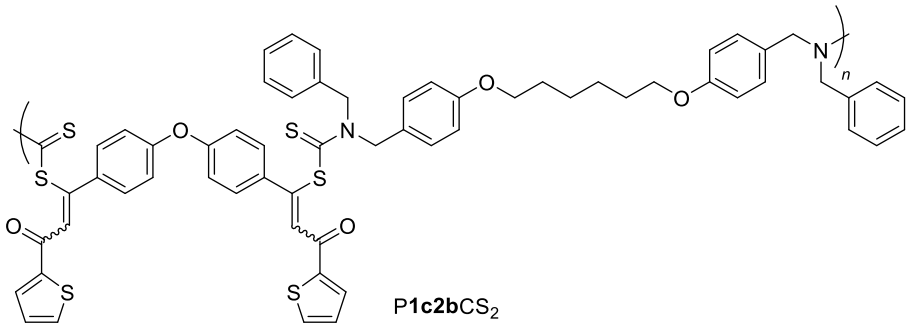

P**1c2b**CS_2

P**1c2b**CS_2. The polymer was obtained as a yellow solid in 97% yield. M_w: 31 400, $Đ$: 1.93. FT-IR (KBr disk), ν (cm^{-1}): 3062, 3031, 2937, 2862, 2194, 1636, 1611, 1588, 1511, 1494, 1470, 1411, 1352, 1242, 1172, 1059, 1012, 965, 924, 857, 830, 727, 698. ^{1}H NMR (400 MHz, DMSO-d_6), δ (TMS, ppm): 8.17 (d, 1.4H), 7.96 (d, 2.6H), 7.68 (d, 4H), 7.52 – 6.65 (m, 26H), 5.04 (d, 8H), 3.85 (s, 4H), 1.64 (s, 4H), 1.37 (s, 4H). ^{13}C NMR (100 MHz, DMSO-d_6), δ (TMS, ppm): 193.85, 181.78, 158.81, 158.64, 157.66, 145.31, 144.70, 136.33, 135.49, 135.04, 134.46, 132.62, 131.10, 129.38, 128.87, 128.24, 127.75, 127.19, 118.89, 115.26, 114.76, 67.83, 56.51, 29.11, 25.80.

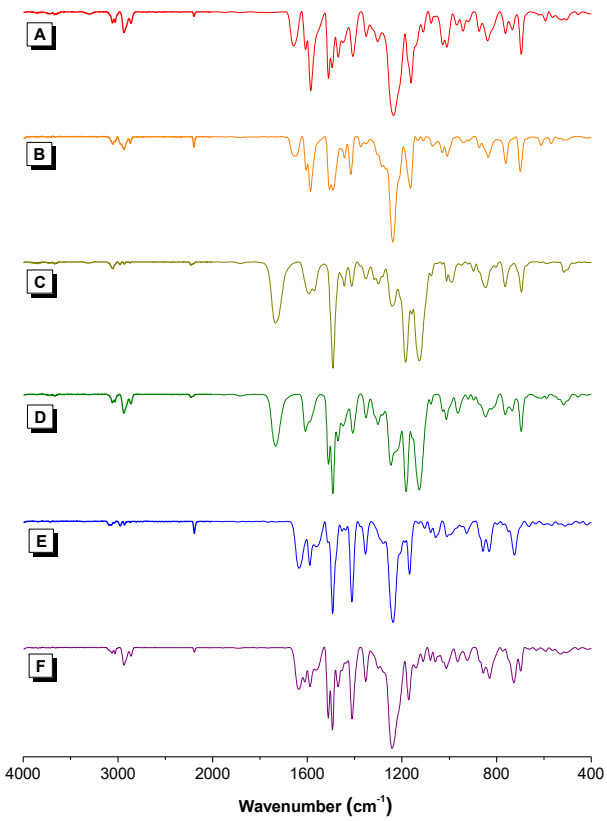

Figure S2. FT-IR spectra of (A) P**1a2b**CS_2, (B) P**1a2c**CS_2, (C) P**1b2a**CS_2, (D) P**1b2b**CS_2, (E) P**1c2a**CS_2, and (F) P**1c2b**CS_2.

FT-IR Spectra of Polymers

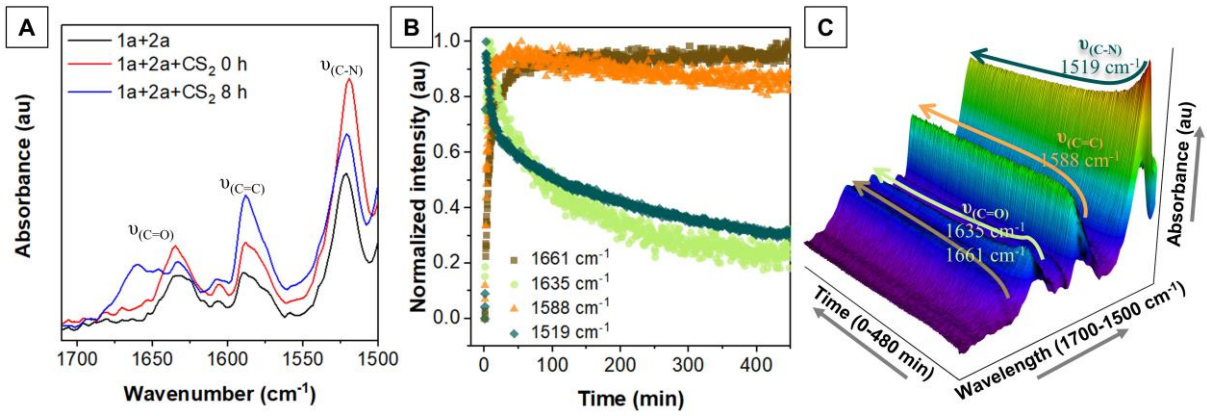

Figure S3. (A) *In situ* IR spectra of the polymerization of P**1a2a**CS_2 in DMSO before and after adding CS_2. (B) Time-dependent peak intensity at 1661, 1635, 1588, and 1519 cm^{-1}, respectively. (C) 3D Fourier transform *in situ* IR profiles of the peaks at 1661, 1635, 1588, and 1519 cm^{-1} for the polymerization of **1a**, **2a**, and CS_2 in DMSO at room temperature.

NMR Spectra of Compound S9 and Polymers

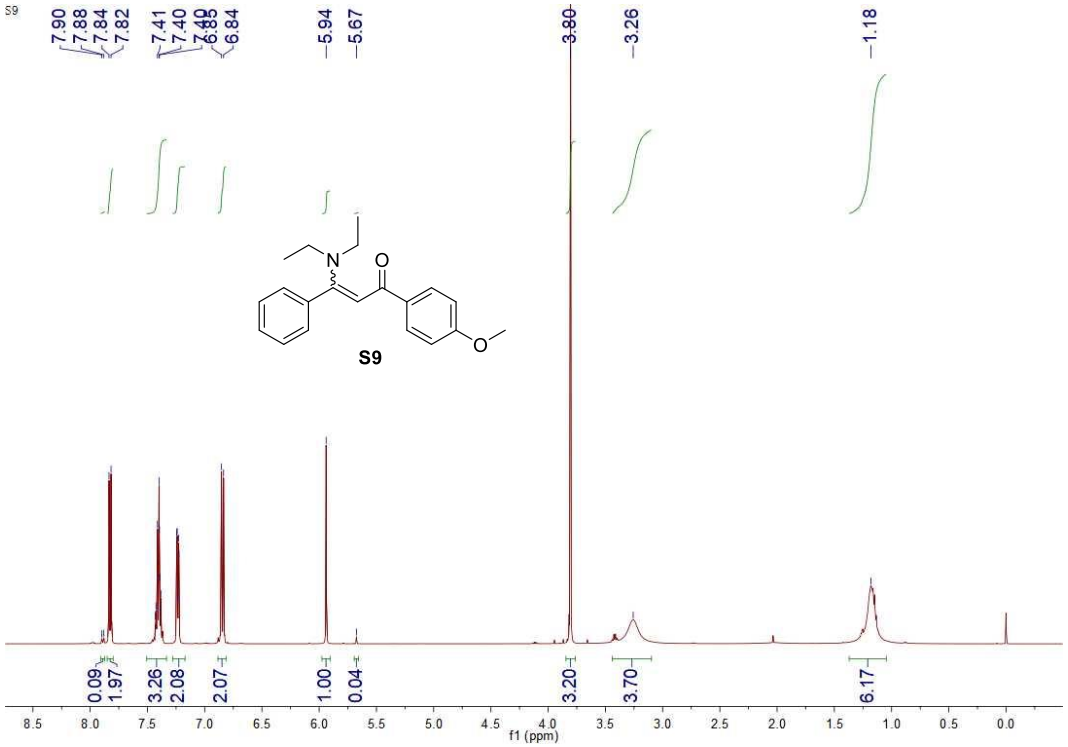

Figure S4. ^{1}H NMR spectrum of **S9** in $CDCl_3$.

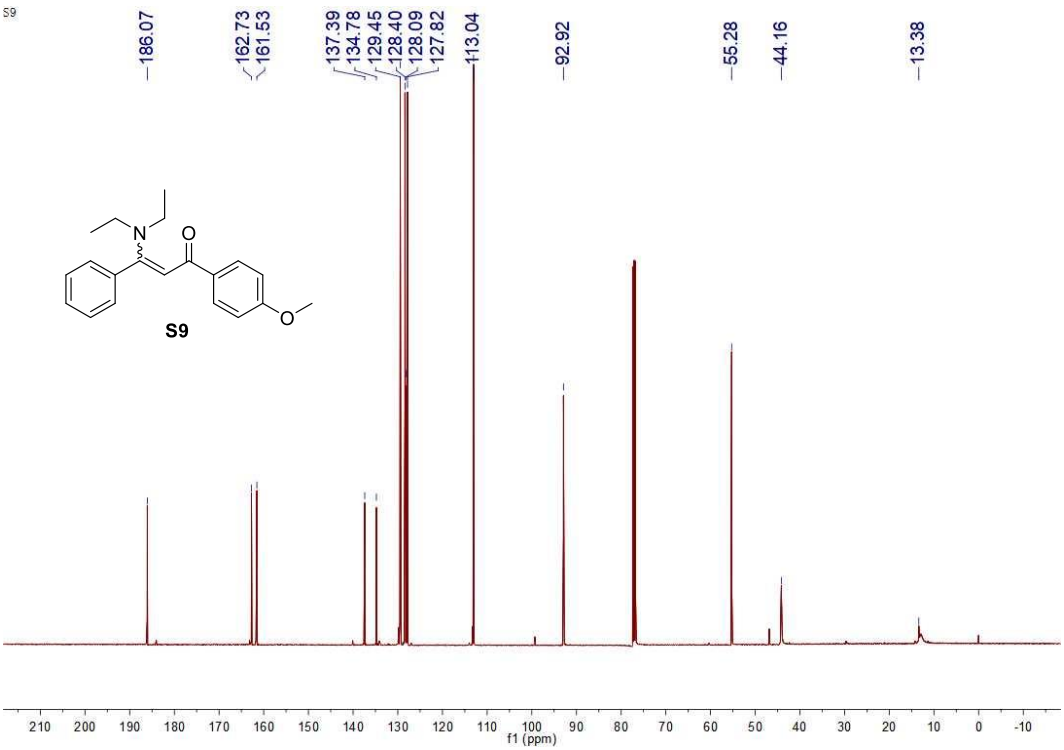

Figure S5. ^{13}C NMR spectrum of **S9** in $CDCl_3$.

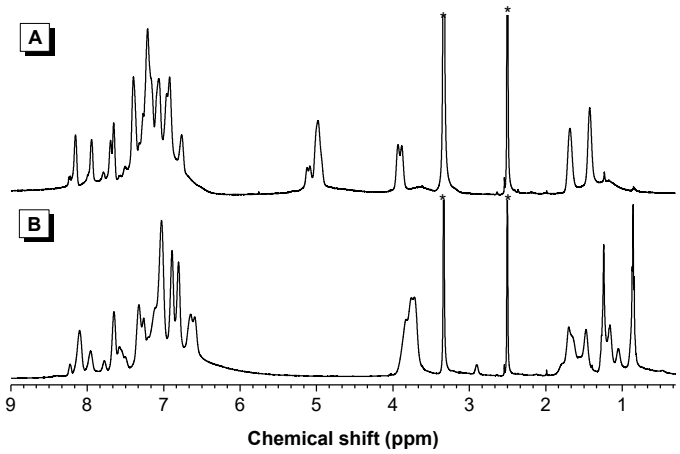

Figure S6. ^{1}H NMR spectra of (A) P**1a2b**CS_2 and (B) P**1a2c**CS_2 in DMSO-d_6. The solvent peaks are marked with asterisks.

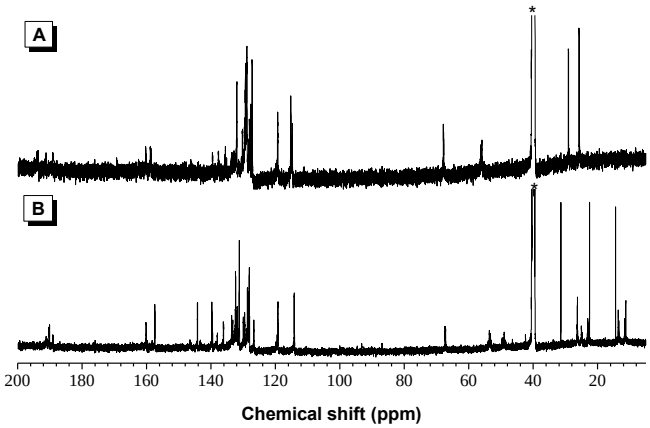

Figure S7. ^{13}C NMR spectra of (A) P**1a2b**CS_2 and (B) P**1a2c**CS_2 in DMSO-d_6. The solvent peaks are marked with asterisks.

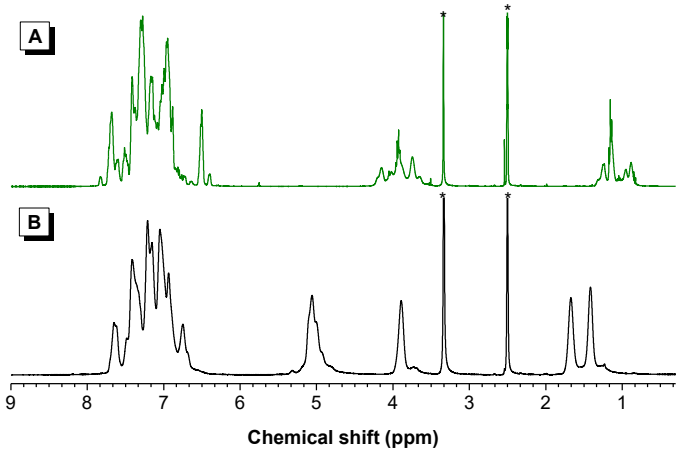

Figure S8. ^{1}H NMR spectra of (A) P**1b2a**CS_2 and (B) P**1b2b**CS_2 in DMSO-d_6. The solvent peaks are marked with asterisks.

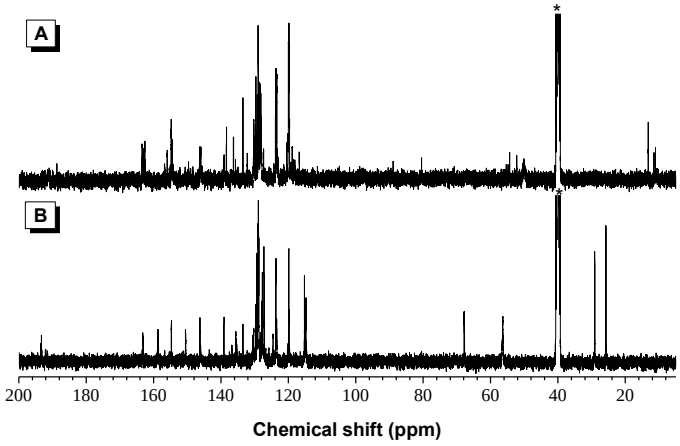

Figure S9. ^{13}C NMR spectra of (A) P**1b2a**CS_2 and (B) P**1b2b**CS_2 in DMSO-d_6. The solvent peaks are marked with asterisks.

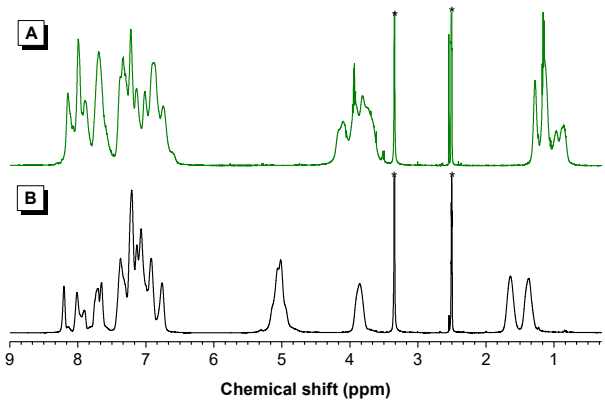

Figure S10. ^{1}H NMR spectra of (A) P**1c2a**CS_2 and (B) P**1c2b**CS_2 in DMSO-d_6. The solvent peaks are marked with asterisks.

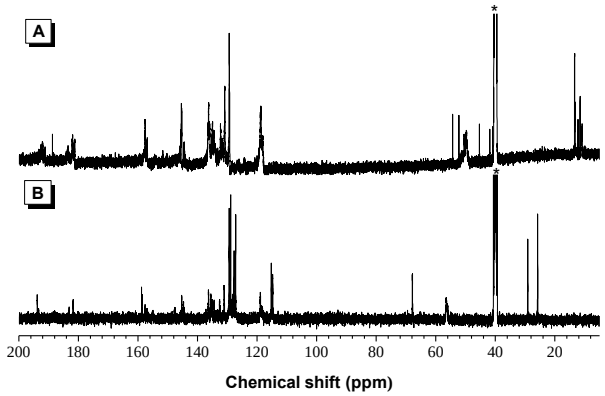

Figure S11. ^{13}C NMR spectra of (A) P**1c2a**CS_2 and (B) P**1c2b**CS_2 in DMSO-d_6. The solvent peaks are marked with asterisks.

Optical Properties of Polymers

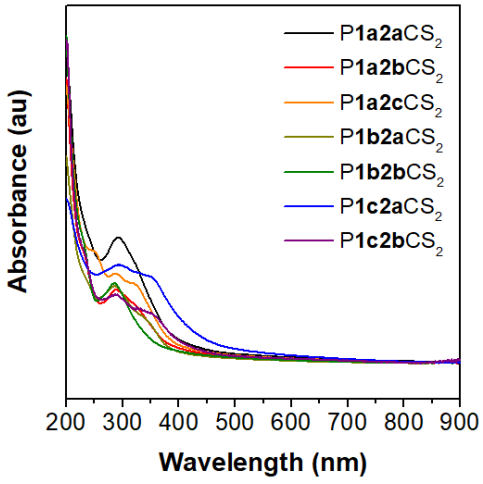

Figure S12. UV-vis spectra of polymer films.

Table S3. The refractive indices and chromatic dispersions of PADDCs.

polymer	$n_{632.8}$	n_{1550}	v_D [b]	v_D' [c]	D [d]	D' [e]
P**1a2a**CS_2	1.6966	1.6594	15.8	82.8	0.063	0.012
P**1a2b**CS_2	1.6575	1.6385	19.7	266.6	0.051	0.004
P**1a2c**CS_2	1.6638	1.6388	15.5	164.1	0.065	0.006
P**1b2a**CS_2	1.6737	1.6291	15.3	67.2	0.065	0.015
P**1b2b**CS_2	1.6712	1.6283	18.5	66.5	0.054	0.015
P**1c2a**CS_2	1.7471	1.6982	9.46	97.3	0.106	0.010
P**1c2b**CS_2	1.6998	1.6525	12.0	73.6	0.083	0.014

[a] Refractive index (n) and dispersion constant of the polymer for different wavelengths are all obtained from the refractive index curve. [b] Abbé number (v_D) = ($n_{589.2}$-1)/($n_{486.1}$-$n_{656.3}$). [c] Corrected Abbé number (v_D') = (n_{1319}-1)/(n_{1064}-n_{1559}). [d] Dispersion of polymers in visible light region (D) = 1/v_D. [e] Dispersion of polymers in infrared light region (D') = 1/$v_{D'}$.

Mechanical Properties of P1a2aCS_2 and Preparation of Ultrathin Membranes

P**1a2a**CS_2 is taken as a representative example to illustrate the process of preparation of the membranes: 100 μL of P**1a2a**CS_2 dissolved with DCM (10 μM) was slowly drop onto a plate of water. Being driven by the surface tension of flowing water, the polymer can spread and float on water, and DCM volatilized at the same time. Following this, the membranes could be transferred to other substrates, for example, silicon or quartz before further characterization.

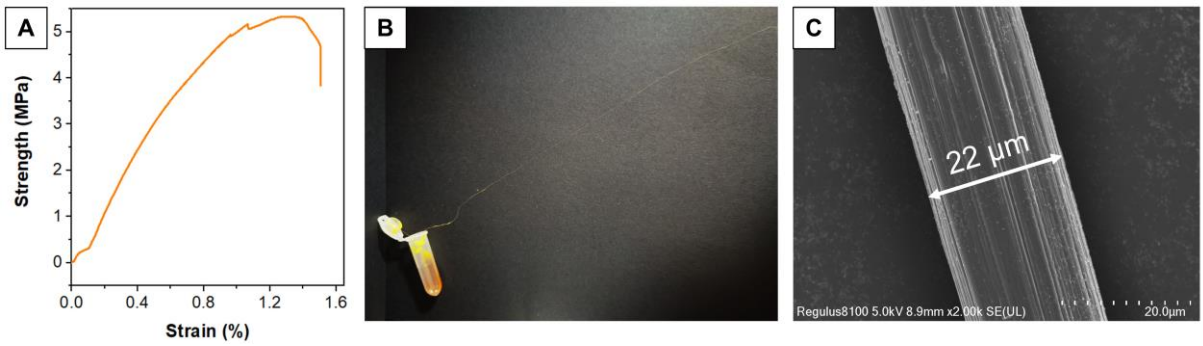

Figure S13. Mechanical properties of P**1a2a**CS_2. (A) The stretch curve of P**1a2a**CS_2 tested by electronic universal testing machine. (B) The continuous fiber of P**1a2a**CS_2 prepared through solution processing and (C) the scanning electron microscope image of this fiber.

References

(1) H. Deng, Z. He, J. W. Y. Lam, B. Z. Tang, Regio- and Stereoselective Construction of Ctimuli-responsive Macromolecules by a Sequential Coupling-hydroamination Polymerization Route. *Polym. Chem.* **2015**, *6*, 8297–8305.

(2) W. Chi, W. Yuan, J. Du, T. Han, H. Li, Y. Li, B. Z. Tang, Construction of Functional Hyperbranched Poly(phenyltriazolylcarboxylate)s by Metal-free Phenylpropiolate-azide Polycycloaddition. *Macromol. Rapid Commun.* **2018**, *39*, e1800604.

(3) B. He, S. Zhen, Y. Wu, R. Hu, Z. Zhao, A. Qin, B. Z. Tang, Cu(I)-catalyzed Amino-yne Click Polymerization. *Polym. Chem.* **2016**, *7*, 7375–7382.

(4) B. Song, B. He, A. Qin, B. Z. Tang, Direct Polymerization of Carbon Dioxide, Diynes, and Alkyl Dihalides under Mild Reaction Conditions. *Macromolecules* **2017**, *51*, 42–48.

(5) B. He, Y. Wu, A. Qin, B. Z. Tang, Copper-catalyzed Electrophilic Polyhydroamination of Internal Alkynes. *Macromolecules* **2017**, *50*, 5719–5728.

(6) X. Chen, T. Bai, R. Hu, B. Song, L. Lu, J. Ling, A. Qin, B. Z. Tang, Aroylacetylene-Based Amino-Yne Click Polymerization toward Nitrogen-Containing Polymers. *Macromolecules* **2020,** *53*, 2516-2525.

(7) B. He, J. Zhang, J. Wang, Y. Wu, A. Qin, B. Z. Tang, Preparation of Multifunctional Hyperbranched Poly(*β*-aminoacrylate)s by Spontaneous Amino-yne Click Polymerization. *Macromolecules* **2020,** *53*, 5248-5254.

(8) V. N. Elokhina, A. S. Nakhmanovich, A. E. Aleksandrova, B. I. Bishnevskii, I. D. Kalikhman, Synthesis and Tuberculostatic Activity of *S*-Acylvinyl-*N*,*N*-dialkyldithiocarbamates and 2-(Diethyliminium)-4-acylmethyl-4-phenyl-1,3-dithietane Perchlorates. *Pharm. Chem. J.* **1986,** *20*, 1061-1063.

Additional Data

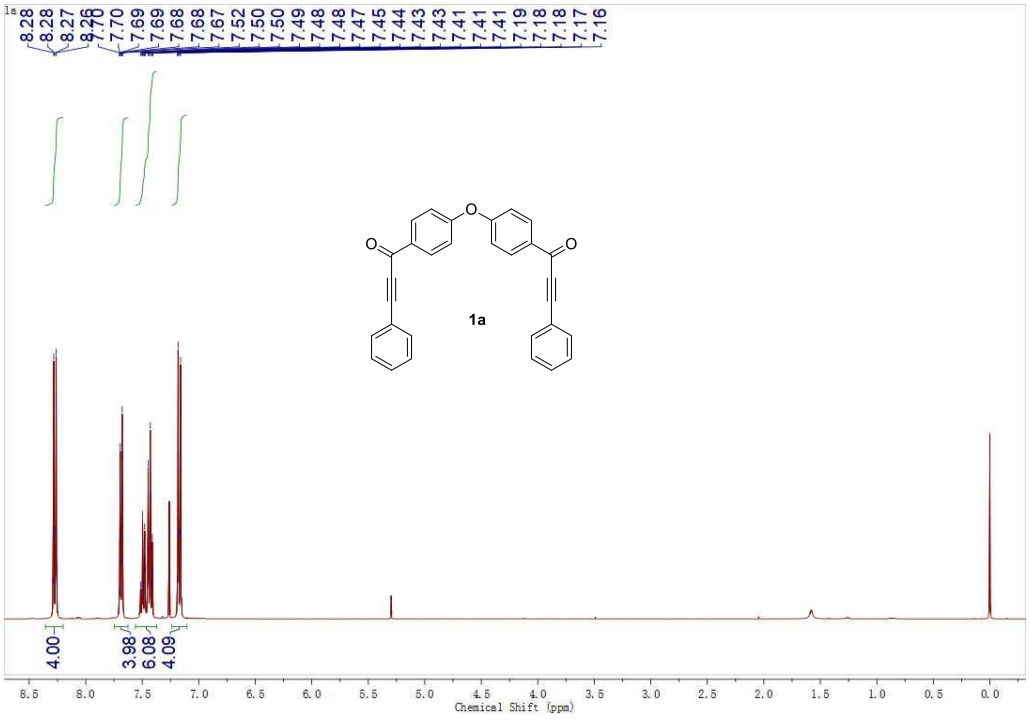

Figure S14. ^{1}H NMR spectrum of **1a** in $CDCl_3$.

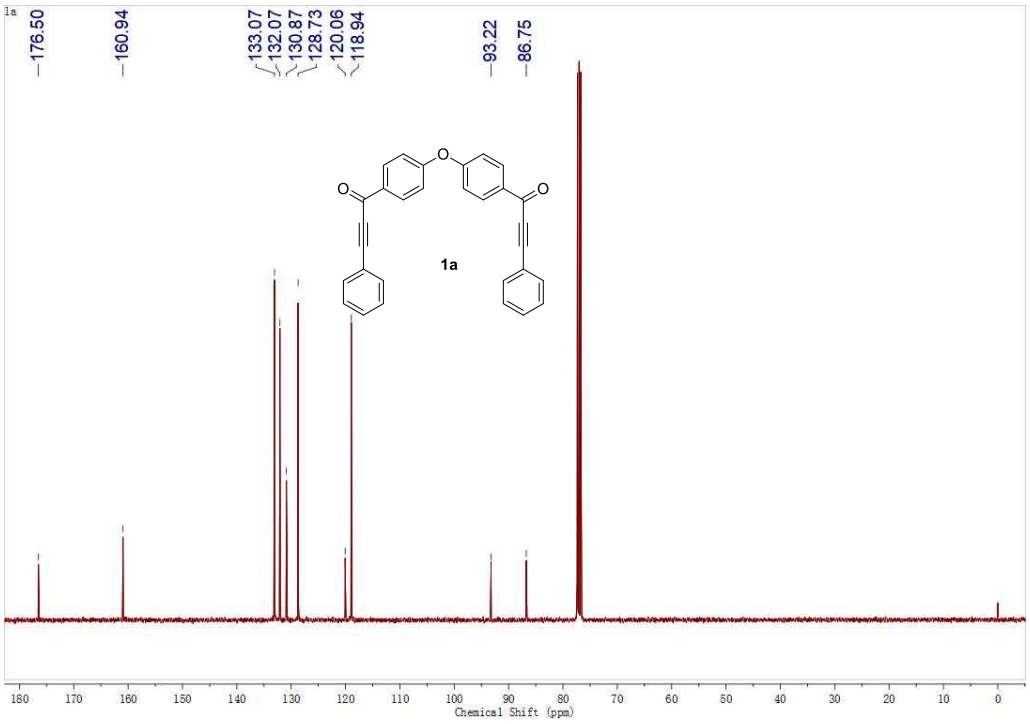

Figure S15. ^{13}C NMR spectrum of **1a** in $CDCl_3$.

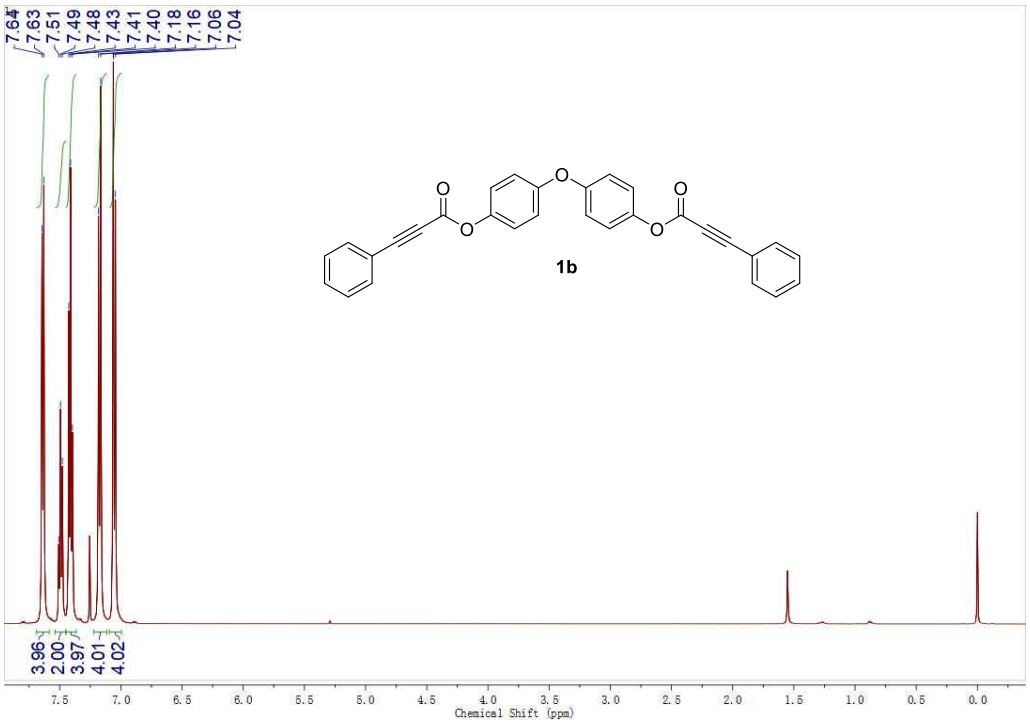

Figure S16. ^{1}H NMR spectrum of **1b** in $CDCl_3$.

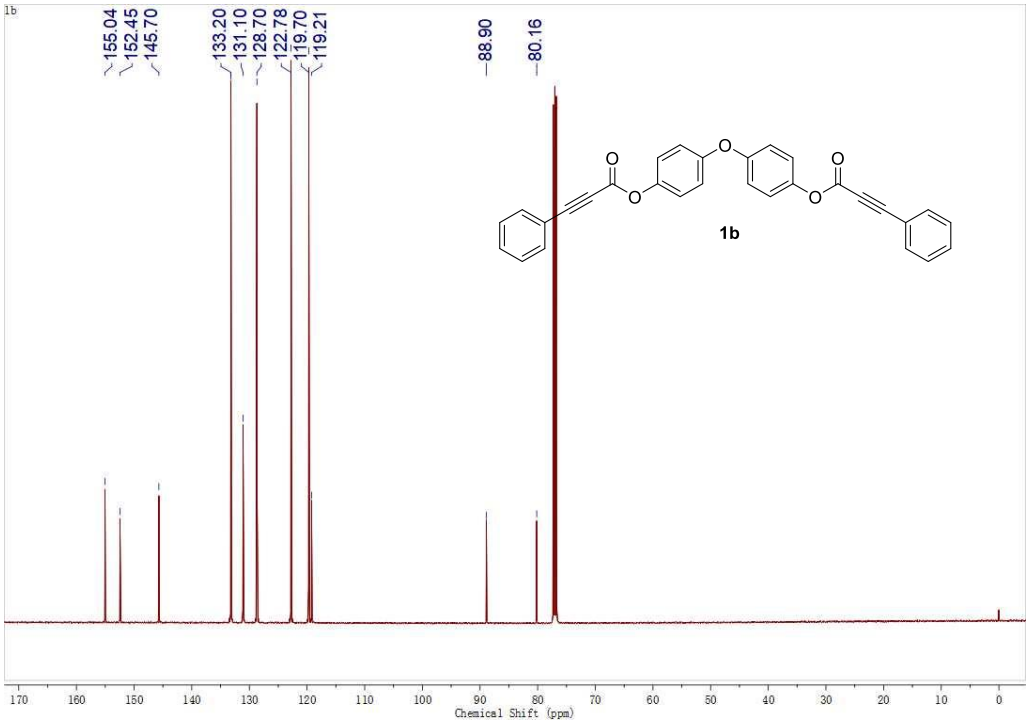

Figure S17. ^{13}C NMR spectrum of **1b** in $CDCl_3$.

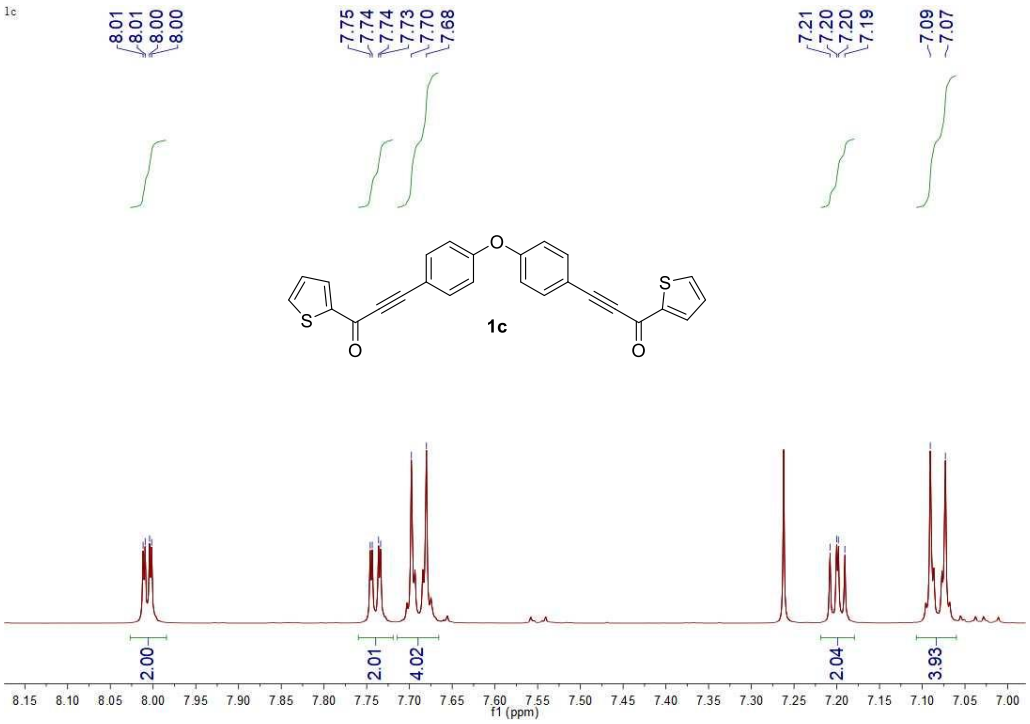

Figure S18. ^{1}H NMR spectrum of **1c** in $CDCl_3$.

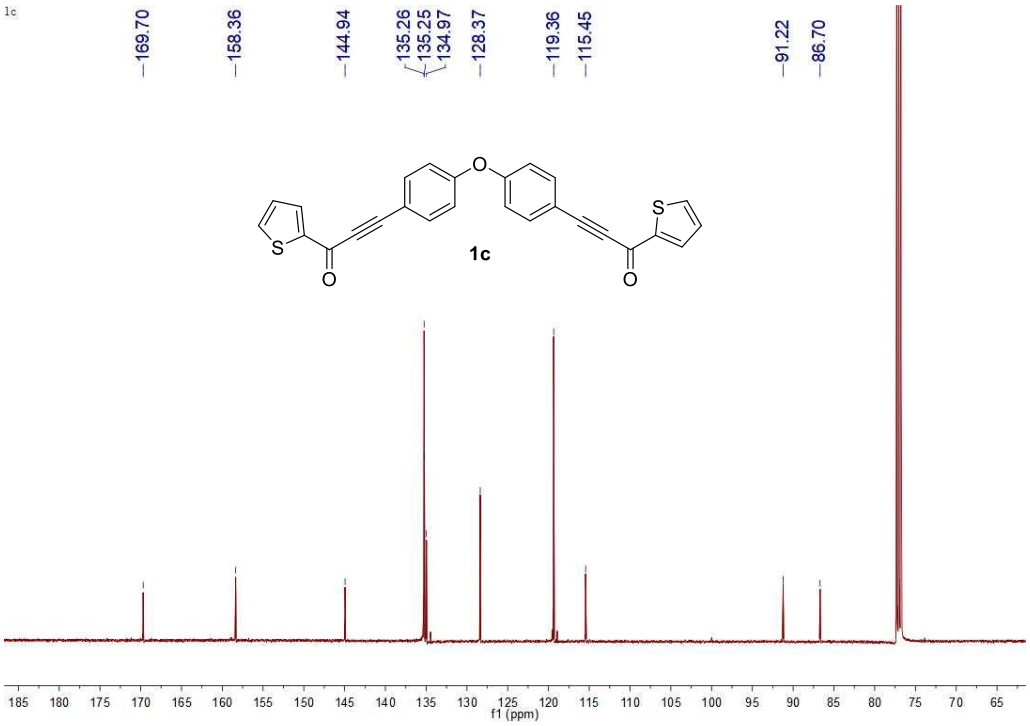

Figure S19. ^{13}C NMR spectrum of **1c** in $CDCl_3$.

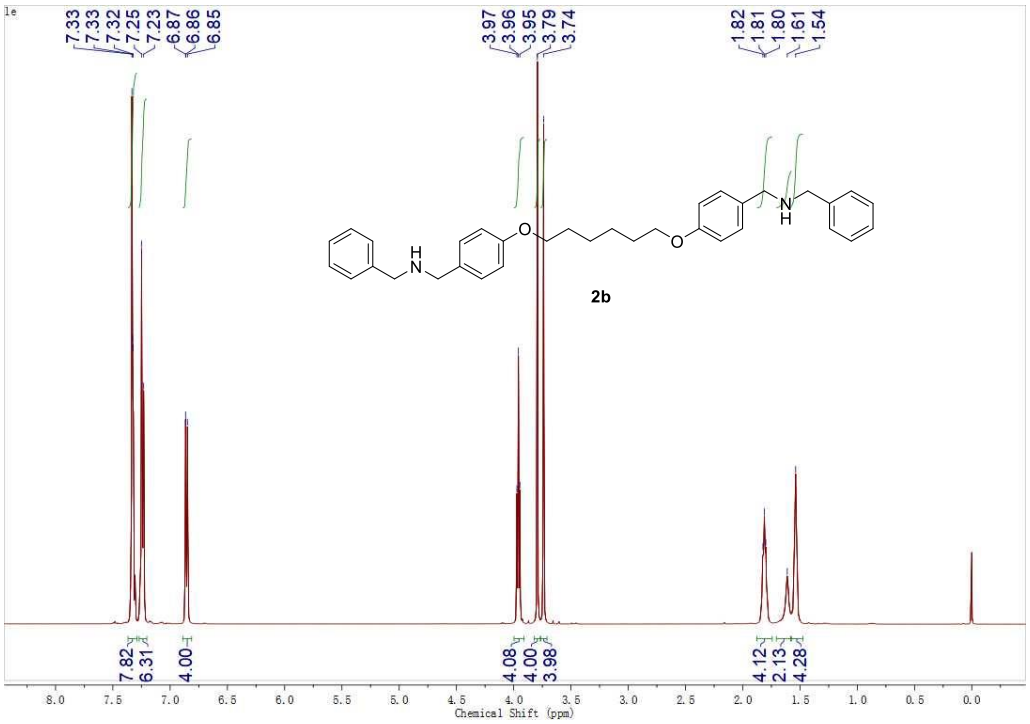

Figure S20. ^{1}H NMR spectrum of **2b** in $CDCl_3$.

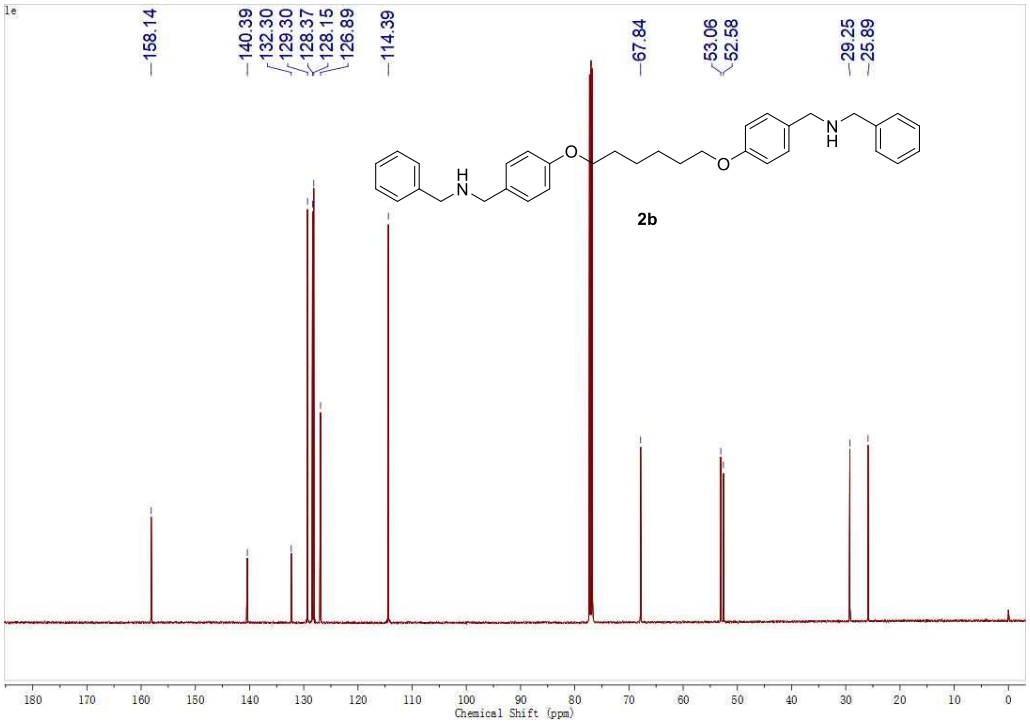

Figure S21. ^{13}C NMR spectrum of **2b** in $CDCl_3$.

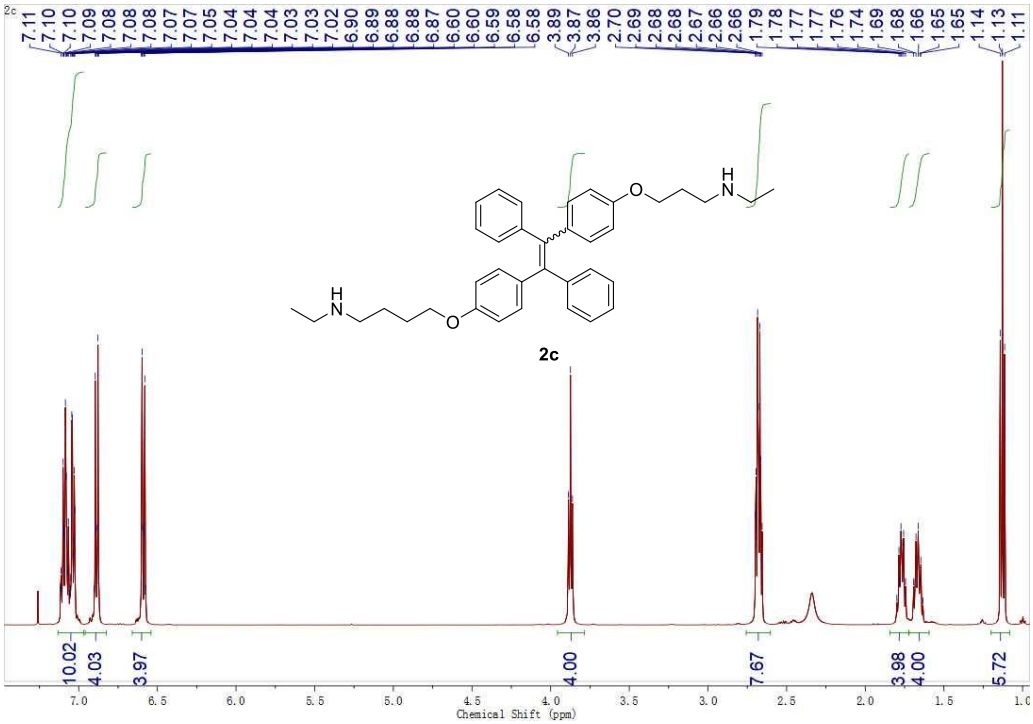

Figure S22. ^{1}H NMR spectrum of **2c** in $CDCl_3$.

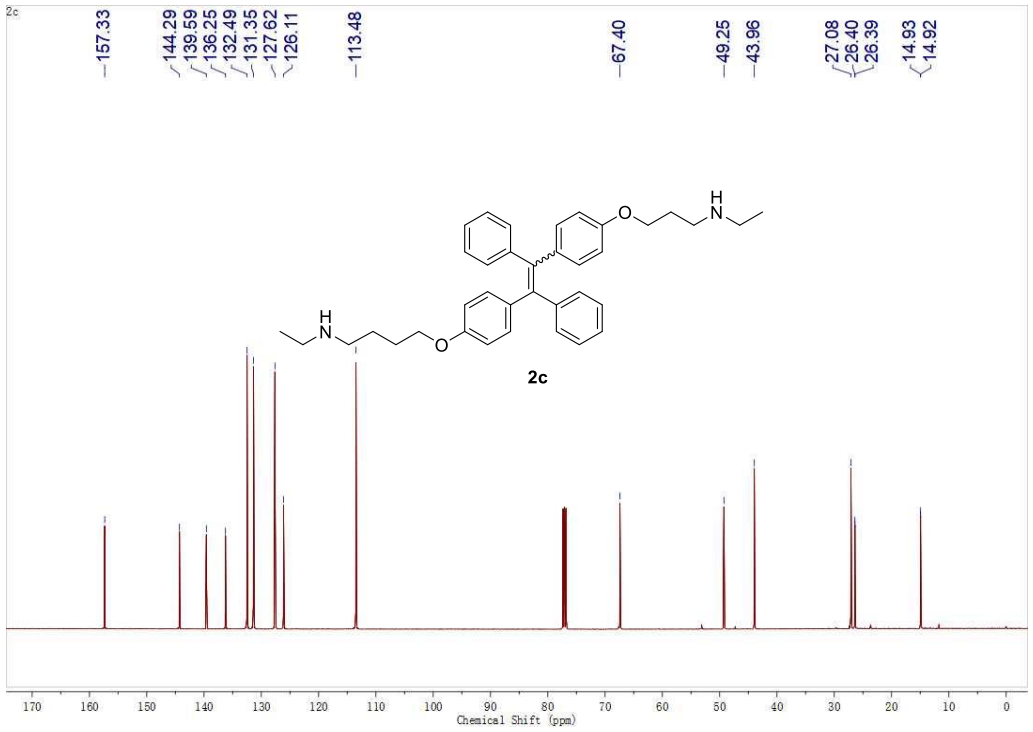

Figure S23. ^{13}C NMR spectrum of **2c** in $CDCl_3$.

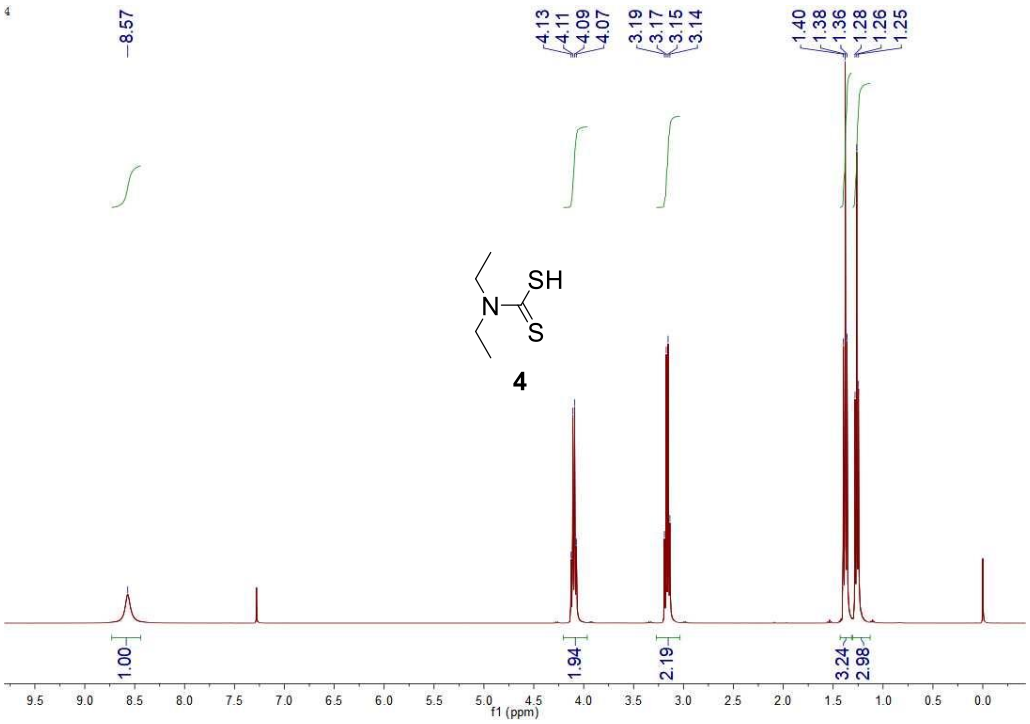

Figure S24. ^{1}H NMR spectrum of **4** in $CDCl_3$.

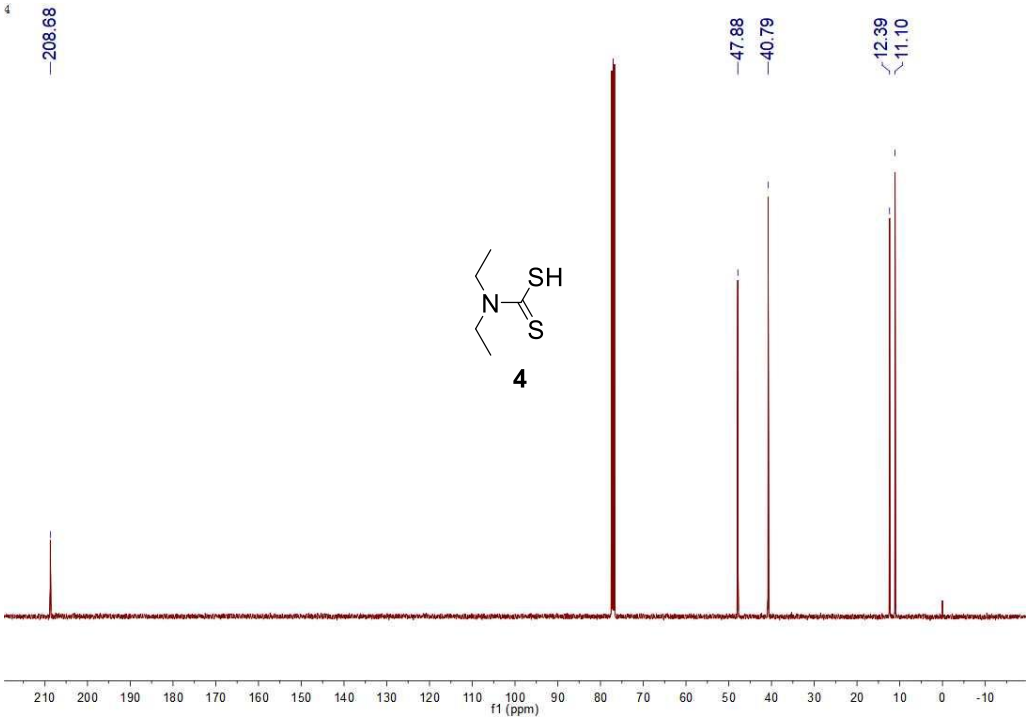

Figure S25. ^{13}C NMR spectrum of **4** in $CDCl_3$.

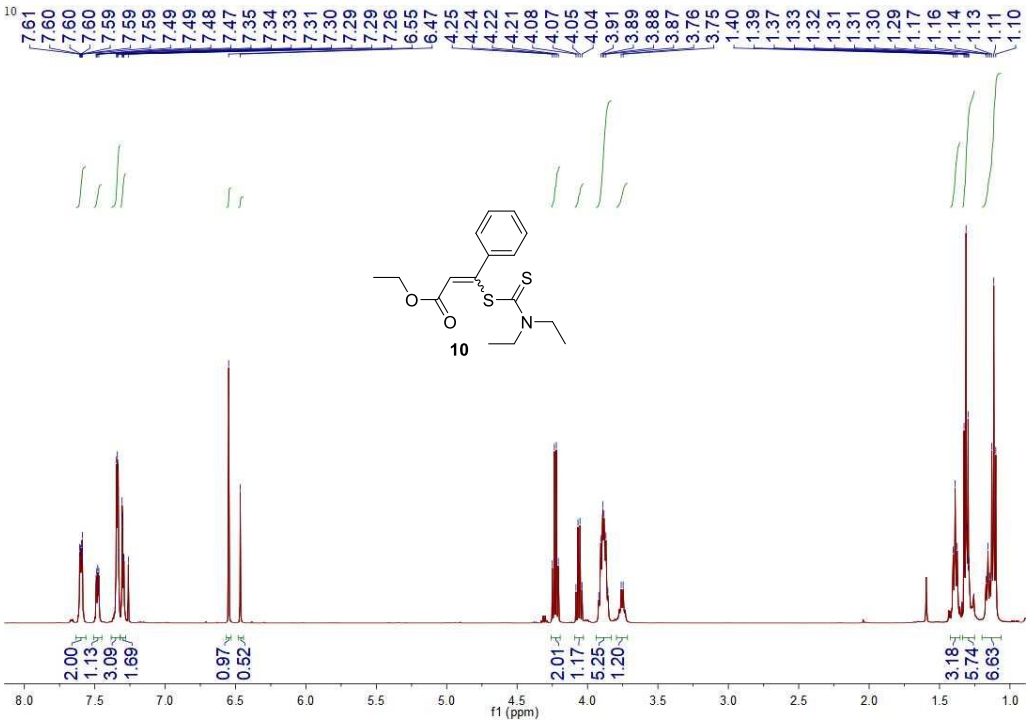

Figure S26. ^{1}H NMR spectrum of **10** in $CDCl_3$.

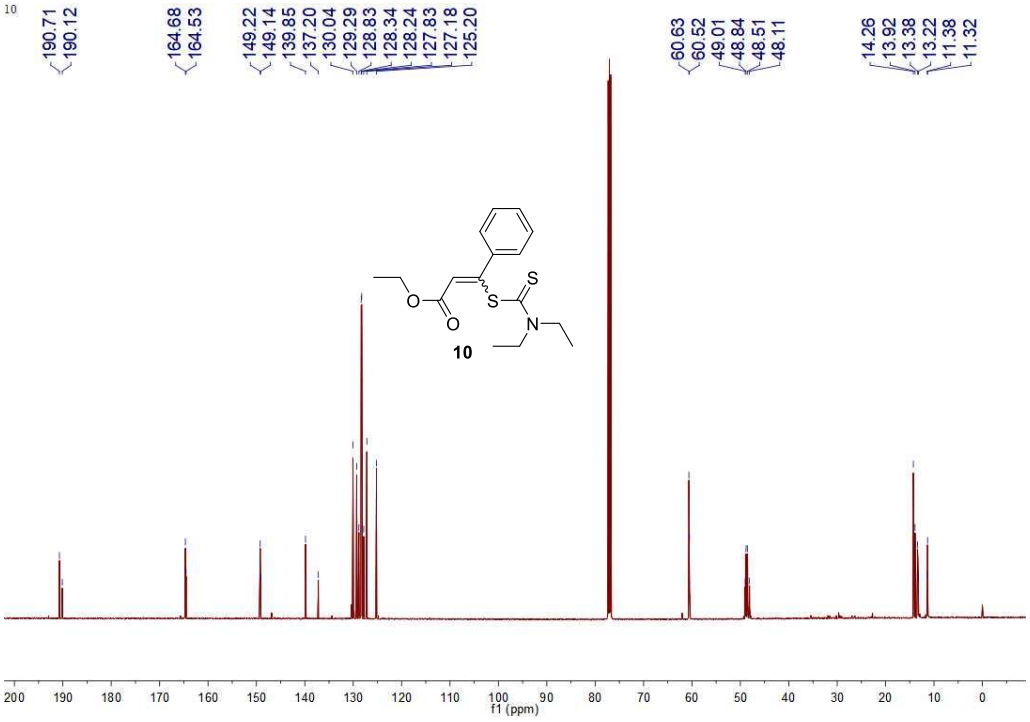

Figure S27. ^{13}C NMR spectrum of **10** in $CDCl_3$.